www.advmatinterfaces.de

# Copper Stress Response of Antibiotic-Resistant and Copper-Tolerant *Enterococcus faecium* and the Antibacterial Efficacy of Functionalized Copper Surfaces

Franca Arndt,\* Katharina Siems, Stella Marie Timofeev, Philippe Baumann, Aisha Saddiqa Ahmed, Daniel Wyn Müller, Frank Mücklich, Aaron Haben, Ralf Kautenburger, Ronja Anton, Christoph Schaudinn, Michael Laue, Oliver Schwengers, Katharina Runzheimer, Rocío Arazo del Pino, Kyriaki Xanthopoulou, Paul G. Higgins, Stefan Leuko, and Alessa Lalinka Boschert

The widespread use of antibiotics worldwide has led to an increase in multi-resistant pathogens, including vancomycin-resistant enterococci (VRE). To prevent the spread of multi-resistant pathogens, antimicrobial surfaces have become more widely used. Various metals and surface topographies are researched to optimize their bactericidal effect. Copper surfaces have proven cost-effective, easy to implement, and safe. However, concurrent metal resistance in Enterococcus faecium, leads to strains highly resistant to both vancomycin and copper. The efficacy of copper coatings are evaluated, and copper and brass surfaces are functionalized with Direct Laser Interference Patterning (DLIP) and determined the release of copper and zinc ions during cell-surface. Additionally, the copper stress response of five E. faecium isolates is characterized by scanning and transmission electron microscopy, determination of the minimal inhibitory concentration (MIC) on copper-infused media, and whole-genome sequencing. The copper stress responses of the isolates differed due to their different copper resistance genes. In particular, it is shown that prior exposure to vancomycin enhanced copper tolerance in E. faecium. Furthermore, the copper-tolerant isolate is the only one to survive direct contact with the functionalized copper surface. These results highlight the importance of investigating antimicrobial and functionalized surfaces against hospital pathogens and co-resistance against metal and antibiotics.

#### 1. Introduction

The global rise of antibiotic resistance poses a significant threat to public health and is associated with an immense economic burden.[1,2] A particularly problematic group is the so-called ESKAPE organisms (Enterococcus faecium, Staphylococcus aureus, Klebsiella pneumoniae, Acinetobacter baumannii, Pseudomonas aeruginosa, Enterobacter-Species), which are prone to develop multi-drug resistance.[3] Many diverse approaches and therapeutic strategies, such as antimicrobial peptides, a combination of antibiotics, bacteriophage, and photodynamic therapies, [4] have been developed as countermeasures. Yet, the risk of transmission, especially via fomites or staff members, remains, potentially resulting in outbreaks within a hospital. Antimicrobial metals like copper and brass, combined with novel surface modifications, have the potential to inhibit the growth and survival of microorganisms in advance to minimize

F. Arndt, K. Siems, S. M. Timofeev, K. Runzheimer, S. Leuko Applied Aerospace Biology Institute of Aerospace Medicine German Aerospace Center Linder Hoehe, 51147 Cologne, Germany E-mail: franca.arndt@dlr.de



© 2025 The Author(s). Advanced Materials Interfaces published by Wiley-VCH GmbH. This is an open access article under the terms of the Creative Commons Attribution License, which permits use, distribution and reproduction in any medium, provided the original work is properly cited.

DOI: 10.1002/admi.202500430

F. Arndt, P. Baumann, A. L. Boschert
Institute for Medical Microbiology
Immunology and Hygiene
University Hospital of Cologne
Goldenfelsstr. 19, 50935 Cologne, Germany
D. W. Müller, F. Mücklich
Chair of Functional Materials
Department of Materials Science
Saarland University
Campus, D3.3, 66123 Saarbrücken, Germany
A. Haben, R. Kautenburger
Department of Inorganic Solid State Chemistry
Elemental Analysis
Saarland University
Campus C4.1, 66123 Saarbrücken, Germany

SCIENCE NEWS

www.advancedsciencenews.com



www.advmatinterfaces.de

infection risk.<sup>[5,6]</sup> With this approach, ESKAPE pathogens like Enterococcus faecium, which can be transmitted via hands and contaminated surfaces, could be eliminated before being transmitted to patients and staff.<sup>[7,8]</sup> Survival on hospital surfaces is a feature of, E. faecium, which is known for its high resilience and desiccation tolerance, lasting up to several months on surfaces in healthcare settings, being desiccation resistant.[9]

Copper surfaces have been shown to effectively reduce bacterial contamination levels in healthcare settings[10,11] with copperalloy surfaces in Intensive Care Units (ICUs) demonstrating significantly lower concentrations of VRE compared to standard surfaces.[12] Moreover, copper has shown effective infection prevention through the use of self-disinfecting beds and significantly lower contamination levels on frequently touched surfaces like handrails and door handles.[10-12] This has led to the incorporation of copper as a critical component in infection control strategies.<sup>[13]</sup> Copper destroys the bacterial cell through several pathways, however, the exact mechanism still remains unclear. Although copper is essential for the general metabolism of bacteria, high concentrations of copper ions are toxic to the cell. Copper ions can bind the bacterial membrane, disrupting its integrity and causing the formation of reactive oxygen species (ROS) on the cell surface, which are highly reactive molecules leading to oxidative stress. [14,15] Copper ions can also catalyze the ROS production through Fenton-like reactions inside the cell, leading to DNA, proteins, and lipid damage. The combination of membrane damage, oxidative stress, protein and DNA dysfunction typically results in irreversible damage and cell death.[15,16]

While these antimicrobial mechanisms are highly relevant for maintaining health on Earth, they are equally important in the context of space travel. Ensuring the health of astronauts and building a microbially safe space environment are both crucial for preventing infections during future long-term spaceflight missions. Studies have evaluated pure and oxidized copper as potential antimicrobial surfaces for spaceflight, highlighting copper

R. Anton Institute for Frontier Materials on Earth and in Space German Aerospace Center (DLR) Linder Hoehe, 51147 Cologne, Germany C. Schaudinn, M. Laue Advanced Light and Electron Microscopy (ZBS4) Robert Koch Institute Seestr. 10, 13353 Berlin, Germany O. Schwengers Bioinformatics and Systems Biology Justus Liebig University Giessen Ludwigsplatz 13-15, 35390 Gießen, Germany R. Arazo del Pino, K. Xanthopoulou, P. G. Higgins Institute for Medical Microbiology Immunology and Hygiene Faculty of Medicine and University Hospital of Cologne University of Cologne Goldenfelsstr. 19, 50935 Cologne, Germany R. Arazo del Pino, K. Xanthopoulou, P. G. Higgins German Center for Infection Research Partner site Bonn-Cologne Kerpener Str. 62, 50937 Cologne, Germany A. L. Boschert MVZ Laboratory Dr. Limbach & Colleagues eGbR Im Breitspiel 16, 69126 Heidelberg, Germany

for preventing microbial growth and biofilm formation in spaceflight environments.[17] Previous studies have explored advanced techniques such as Direct Laser Interference Patterning (DLIP) with ultra-short pulses (USP) to modify surface topography and enhance antimicrobial properties, demonstrating that micro- and nano-structured surfaces can significantly inhibit bacterial adhesion and growth.[6,18]

This method is expected to reduce microbial load and biofilm formation more effectively than smooth surfaces, as investigated in the spaceflight experiment BIOFILMS.<sup>[19]</sup> Furthermore, these surfaces were recently also investigated for their antifungal efficacy.[20] These functionalized materials are a promising solution against pathogens, reducing microbial load and preventing biofilm formation, providing a long-term solution to surface contamination. [6,19] Hence, they may also prove to be valuable solutions for preventing contamination in hospital settings. Furthermore, thin copper coatings are an option to prevent the spread of bacteria on hand-touch sites in spacecrafts, as they can be applied on various surfaces and have already been shown to reduce bacterial loads on frequently touched surfaces in healthcare environments. [21,22] Various techniques exist for applying copper coatings. Coatings applied by sputtering have several advantages, such as providing a homogeneous coating with high adhesion and dense deposits on flat substrates.<sup>[23]</sup> In addition, the coatings are of high purity as the deposition takes place in a high vacuum. As magnetron sputtering is considered a cold deposition technique with little radiant heat, it can be applied not only to metals, ceramics, and glasses, but also to heat-sensitive polymerbased materials.[24] Moreover, coatings are more sustainable because fewer critical resources, such as copper, are required, and they can be reapplied when needed.[13] Overall, the application of copper coatings offers great potential for infection control in healthcare settings, particularly high-touch surfaces.<sup>[25]</sup>

Despite the demonstrated antimicrobial properties of copper, there is growing concern about the potential for bacteria to develop resistance to metals. The according resistance genes are often located on mobile genetic elements, facilitating their transfer between bacteria within and from different ecosystems.<sup>[26]</sup> The presence of critical copper concentrations in the environment, alongside antibiotic resistance genes in bacterial genomes, suggests that using copper as an antimicrobial surface could potentially select for multi-drug-resistant strains.[27-29] Animal farming has a significant implications and an underestimated role for the development and spread of combined copper and multidrugresistant bacteria.[30] For example, copper tolerance is emerging alongside antibiotic resistance in Enterococci found in pig farms, where copper is used as a growth supplement.[31] The European Food Safety Authority (EFSA) Panel on Additives and Products or Substances used in Animal Feed recommended a maximum of 25 mg kg<sup>-1</sup> feed, however, the EU regulation on copper sources for animal nutrition allows 150 mg kg<sup>-1</sup> feed for young piglets.[32,33] The use of copper in pig farming has been linked to the rise of copper-tolerant bacteria, such as isolates like the E. faecium strain A17sv1, which was isolated from pig feces and is resistant to several antibiotics, including vancomycin.[34] This strain harbors acquired copper resistance, mediated by the transferable copper resistance (tcrB) gene, which encodes an efflux pump, a protein belonging to the CPx-type ATPase family.[34] Due to the co-localization of resistance genes on the same



www.advmatinterfaces.de

plasmid, *tcrB* co-selects for antibiotic resistance, including gly-copeptide resistance in *E. faecium*.<sup>[35,36]</sup> Regular copper homeostasis in Enterococci is regulated by the *cop* operon, which encodes, among others, for *copA* (influx) and *copB* (efflux), ATP-dependent pumps that regulate copper intake in the cell.<sup>[37]</sup>

Overall, there is a fine line to use copper as an antibacterial surface against VRE, managing the co-occurrence of copper and antibiotic resistances in animal farming, which potentially poses a risk to public health.[38] This delicate balance is crucial because improper use of copper could be harmful by promoting the emergence and spread of multi-resistant bacterial strains.[13] The dual challenge of copper exposure in hospitalacquired pathogens may actively contribute to the selection and maintenance of multidrug-resistant Enterococci and other pathogens through the co-transfer of copper resistance genes alongside resistance genes against first-line antibiotics via mobile genetic elements. Silveira et al. (2023) analyzed 922 Enterococcus isolates from different environments (humans, animals, environment, food), showing widespread copper-tolerance genes (tcrB and cueO) and describing the co-transfer of those along with ampicillin resistance for the first time. [39] This study highlights the potential risk of using copper-based materials in hospitals, thus promoting the selection of multidrug-resistant pathogens.

Despite the promise of antibacterial functionalized surfaces, there is a notable gap in research regarding their effectiveness, specifically against copper-tolerant bacteria. This study aims to evaluate the efficacy of functionalized DLIP-USP copper and brass surfaces, with 3 µm topography, in combating antibiotic-resistant and copper-tolerant *E. faecium*. By analyzing resistance genes from both clinical and animal isolates, we aim to gain a comprehensive understanding of resistance genetics and the potential impact of copper as an antimicrobial surface in managing resistant pathogens.

#### 2. Results and Discussion

#### 2.1. Bacterial Survival on Functionalized Surfaces

The samples (copper, brass, stainless steel) were structured with a periodic 3 µm line pattern using Direct Laser Interference Patterning (DLIP) with ultrashort pulses (USP). In DLIP, the periodicity of the pattern (P) is determined by the laser wavelength ( $\lambda$ ) and the interference angle ( $\theta$ ) according to P =  $\lambda$  / (2·tan  $\theta$ ). For a periodicity of 3 µm, a setting of  $\theta$  = 7.66° was used. Such microstructured surfaces, as demonstrated in previous studies, can significantly influence bacterial adhesion and growth, thereby enhancing the antimicrobial properties of copper. [6.18,40,41]

The type strain (DSMZ 20477<sup>T</sup>) displayed a stable survival on both smooth and patterned steel at all time points, while viability decreased significantly on copper and brass surfaces: after 15 min on smooth copper and brass, 30 min on patterned brass and patterned copper showed an over 3-log reduction after 45 min (**Figure 1A**). Although there were no statistically significant differences between smooth and patterned surfaces, all brass and smooth copper surfaces demonstrated significantly greater antimicrobial activity than steel (smooth steel/smooth copper p < 0.05; smooth steel/smooth brass p < 0.05; patterned steel/patterned brass p < 0.001).

For the reference strain (DSMZ 17050) no reduction in survival was detected after 60 min on smooth steel. However, the survival on smooth steel was significantly different from patterned steel (p < 0.001, Figure 1B). No survival was detected on smooth copper after 15 min, while patterned copper caused an over 3-log reduction after 45 min. The strain survived for 30 min on patterned brass and 60 min on smooth brass. Overall, copper and brass surfaces (smooth and patterned) reduced survival compared to steel, with smooth copper and patterned brass showing the strongest antimicrobial effect. Brass surfaces and patterned copper were significantly different from the steel reference (smooth steel/smooth brass p < 0.001; patterned steel/patterned brass p < 0.05; patterned steel/patterned copper p < 0.001, Figure 1B).

The clinical isolate (VRE-13) showed stable survival across all timepoints on both steel materials (Figure 1C). The strongest antimicrobial effect was observed after 15 min on smooth brass and after 30 min on smooth copper. Patterned copper and brass led to no survival after 45 min. Significant differences were observed for copper compared to steel (smooth steel/smooth copper p < 0.05, patterned steel/patterned copper p < 0.05) as well as for patterned brass (p < 0.05). Bacterial survival lasted significantly longer on patterned brass compared to smooth brass (p < 0.05). Figure 1C).

The clinical isolate (VVE-B-19) showed stable survival on smooth steel for 60 min and a slight increase on structured steel (Figure 1D). The strongest antimicrobial effect was observed after 15 min on smooth and patterned copper and smooth brass, while the isolate persisted up to 30 min on patterned brass. The surface topography had a significant effect, resulting in a lower antimicrobial impact compared to patterned brass after 15 min (p < 0.05, Figure 1D).

The copper-tolerant isolate A17sv1 showed high survival on all tested materials up to 60 min, with the highest reduction on smooth copper (3-log reduction). Patterned copper had a significant effect compared to steel (p < 0.001, Figure 1E), but smooth copper was significantly more effective against the A17sv1 isolate than the patterned copper (p < 0.05). A reduction in survival was observed on patterned brass, followed by smooth brass, though patterned brass showed almost no effect after 60 min. Smooth brass had a significantly higher antimicrobial effect than patterned brass (p < 0.05, Figure 1E).

Overall, the antimicrobial effect of copper and brass is in line with our findings, which showed a reduction in survival across all tested isolates. [15] To enhance the antibacterial effect, copper and brass materials processed by USP-DLIP have shown a 99% (2log) reduction in viable E. coli cells within 15 min, while smooth copper surfaces reached a similar reduction after 60 min.<sup>[6]</sup> In contrast, we observed an enhanced antibacterial effect on smooth rather than on USP-DLIP surfaces. One possible explanation is that the increased surface area and microscale roughness could provide better opportunities for bacteria to adhere efficiently, [42,43] potentially supporting biofilm formation, allowing bacteria to survive longer on patterned surfaces. However, it was shown that the retention can be significantly reduced on DLIP-processed surfaces in E. coli and S. aureus. [44] This suggests that the effectiveness of DLIP surfaces depends strongly on the specific topography, scale, and bacterial species involved. In particular, the shape of the bacterial cells (e.g., rod-shaped vs. cocci) and the dimensions of the surface topography, such as the groove spacing

21967350, 0, Downloaded from https://adv

, Wiley Online Library on [10/09/2025]. See the Terms

on Wiley Online Library for rules of use; OA articles are governed by the applicable Creative Commons License

www.advancedsciencenews.com

**ADVANCED** SCIENCE NEWS

www.advmatinterfaces.de

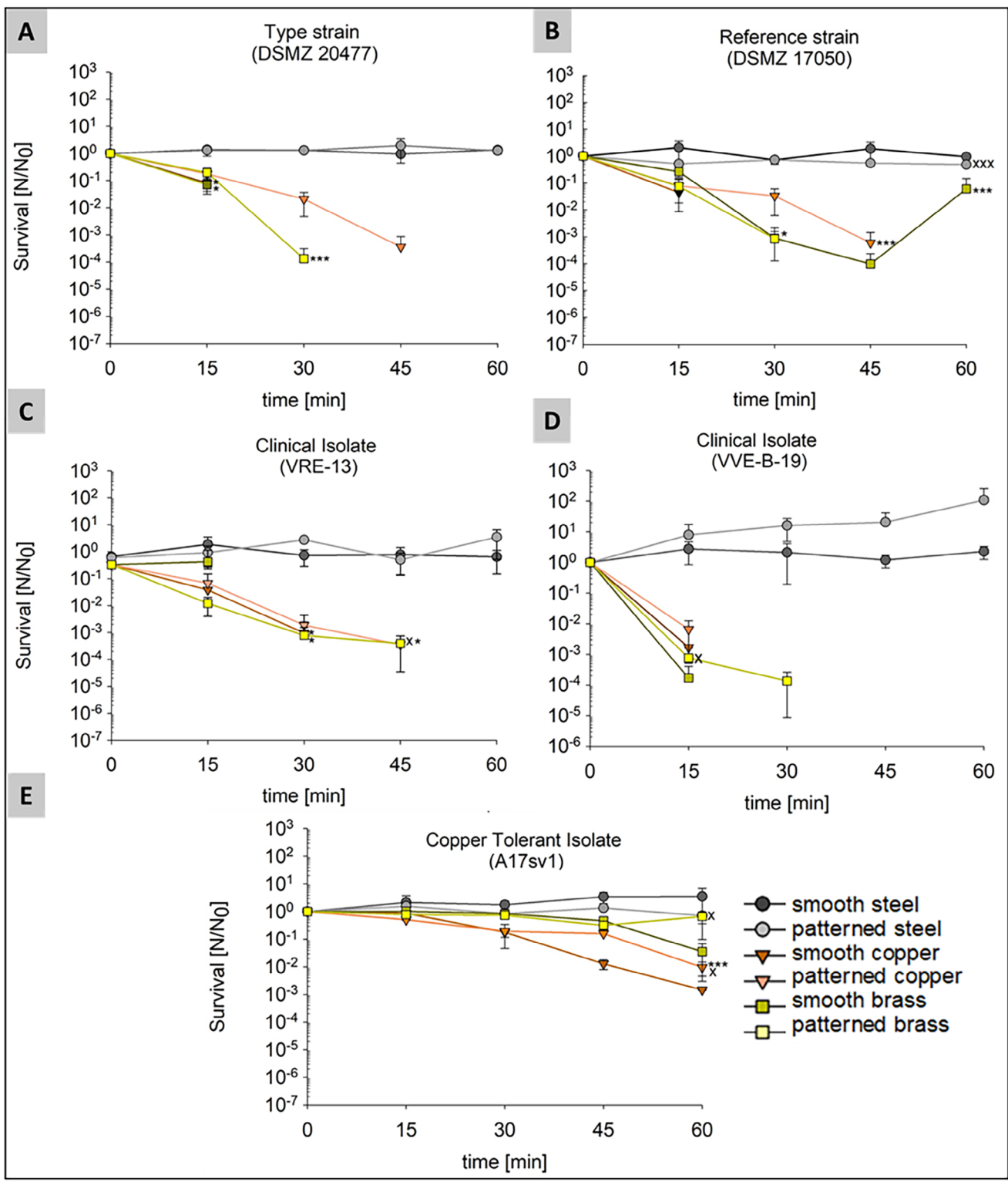


**Figure 1.** Survival data (N/N<sub>0</sub>) of *E. faecium* (**A** type strain DSMZ 20477<sup>T</sup>, **B** reference strain DSMZ 17050, **C** clinical isolate VRE-13, **D** clinical isolate VVE-B-19, **E** copper-tolerant isolate A17sv1) after contact to different metal surfaces for 15, 30, 45, and 60 min. (N number of surviving colony-forming units (CFUs) at a given time point; N<sub>0</sub> is the initial number of CFUs at the start of the experiment). Surface types: smooth steel, patterned steel (3 μm USP-DLIP), smooth copper, patterned copper (3 μm USP-DLIP), smooth brass, patterned brass (3 μm USP-DLIP). Measurements were performed in triplicate, and calculated error bars show the standard deviation of each sample (n = 3). Significance was determined by two-sample t-test; the conditions corresponding to the significance levels are as follows: significant to steel/control reference p = 0.05, p = 0.001, significance between smooth and patterned surfaces of the same material (smooth/patterned) p = 0.05, p = 0.001.





www.advmatinterfaces.de

relative to bacterial size, can significantly influence bacterial survival on patterned surfaces. [43] In our study the 3 μm topography used is larger than the size of cocci (0.5-1 µm), which may not have provided optimal conditions for an efficient inactivation of bacteria. Previous research has shown that topographic micronsized features, which match the size of bacteria, can enhance attachment, whereas nano-sized features reduce it.[6,45,46] Additionally, cell-cluster agglomeration was observed on 3 µm patterned surfaces for S. aureus, which may have a protective effect, as clustered cells have less direct contact with the surface compared to single cells.[47] Thus, further testing with surfaces patterned with a topography of 280 nm is necessary to compare the antimicrobial effect and smaller topographic features, which could provide increased bacterial contact area.<sup>[47]</sup> This, however, also poses an immense challenge: Since the surface microbiota consists of bacteria of varying size and shape, there remains the risk of selection when deciding on specific topographic size.

Additionally, the surface microbiota consists of Gram-negative and Gram-positive bacteria, which differ in their handling of copper uptake due to differences in cell structure. Although Gram-negative bacteria like E. coli possess an additional outer membrane and a periplasmic space that could theoretically delay copper uptake, the study found that E. coli was killed more rapidly than E. faecium, [48] suggesting that the thick peptidoglycan layer in Gram-positive bacteria may provide additional protection.[47-49] While our study focused only on Gram-positive E. faecium, there are important methodological differences to consider. For example, the referenced study[48] used a higher initial cell number (1–1.4  $\times$  10<sup>7</sup> CFU), which may have resulted in multilayered cell clusters that could protect inner cells from direct surface contact. In contrast, our experiments used a lower starting concentration (6.0  $\times$  10<sup>4</sup> CFU), ensuring  $\approx$ 99% monolayer on the tested surfaces (diameter 6 mm), thus allowing for more direct cell-surface interaction. Hence, testing both Gramnegative and Gram-positive bacteria, along with factors such as starting cell number and experimental design, can significantly influence bacterial survival outcomes.

Furthermore, bacterial survival is impacted by whether the cells are under dry or wet conditions during the contact-surface time, with a faster reduction in survival under dry conditions. However, this also varies depending on the bacterial species. [48,14] We observed a 3-log reduction of the copper-tolerant strain (A17sv1) after 60 min of contact with the copper surface, tested under wet conditions. Previous research reached a 6-log reduction within the same time and an even faster killing effect during dry conditions. [14] This could be due to the direct contact with the surface of the cell, which cannot dilute high intracellular copper concentrations with surrounding liquid. Therefore, testing under dry conditions may better reflect real-world surface transmission, such as in hospital environments, and should be considered in future studies.

Previous studies have suggested that copper exposure in the environment may co-select for multidrug-resistant enterococci. [26,28,39,50] However, in our study, no clear correlation was observed between vancomycin resistance and survival on copper among the five tested isolates. For example, the vancomycin-susceptible type strain (DSMZ 20477T) survived 45 min on patterned copper just as well as the vancomycin-resistant reference strain (DSMZ 17050) and the clinical isolate

(VRE-13). These findings indicate that vancomycin resistance alone may not predict copper tolerance, emphasizing the need for a higher isolate number has to be tested to gain deeper insights into a copper tolerance and vancomycin resistance correlation.

In general, copper is essential to bacterial copper homeostasis and is regulated by the cop operon (copYZAB) in E. hirae.[37] Within the copper homeostasis, zinc is an important co-factor, which is bound to the CopY repressor, preventing the expression of the copper efflux genes. If copper accumulates inside the cell during direct surface-cell contact, the copper-responsive repressor CopY dissociates from the promoter, and gene expression for the cop operon is induced. This activates the efflux system, including CopB, a CPx-type ATPase pump that transports copper out of the cell.[37,51] Based on our results, we conclude that direct contact with copper surfaces, combined with dissolved copper ions in the cell suspension, leads to intracellular copper accumulation that overwhelms the efflux system in Enterococci, disrupting copper homeostasis. Zinc itself has an antibacterial activity, [52,53] but also plays an essential role in binding to Copy. However, it does not improve the survival of Enterococci on brass surfaces (Zn 37% and Cu 63%) or prevent the copper ion overload, especially at high copper concentrations. This is in line with our results, as most bacterial isolates exhibited a significantly reduced survival after 30 min of contact with brass. To address copper corrosion and its longevity regarding its antibacterial effect, long term-experiments must be conducted to fully assess the antimicrobial efficacy of copper surfaces, which has a significant impact on bacterial killing.[48,54]

### 2.2. Cu and Zn Ions Release Rate Measurement

As expected, no copper or zinc ions were detected in the cell suspension after contact with the steel reference (Figure 2). The copper ion concentrations after the wet-contact killing experiment with the type strain (DMSZ 20477<sup>T</sup>) correlated with the survival data. In this case, the strain showed the lowest survival on the smooth copper surface, which exhibited the highest antibacterial activity (see Figure 1A). This aligns with the elevated copper concentrations observed in the cell suspension (compare Figure 2A). On brass, copper concentrations ranged from 12.65  $\mu g \ L^{-1}$  (smooth) to 17.53  $\mu g \ L^{-1}$  (patterned). After 15 min, patterned brass released significantly more copper than smooth brass (p < 0.01, Figure 2A). Overall, copper concentrations increased over time in both strains, ranging after 60 min from 23.3  $\mu g L^{-1}$  (patterned copper) to 28.1  $\mu g L^{-1}$  (smooth copper). For the type strain (DMSZ 20477<sup>T</sup>) significantly higher copper ion levels were measured on smooth compared to patterned copper at 15 min (p < 0.001), 30 min (p < 0.01), and 45 min (p < 0.001, Figure 2A). On brass, the copper concentration ranged from 12.65  $\mu g \ L^{-1}$  (smooth) to 17.53  $\mu g \ L^{-1}$  (patterned). After 15 min, patterned brass released significantly more copper than smooth brass (p < 0.01, Figure 2A).

For the copper-tolerant strain (A17sv1) the copper ion concentrations during the wet-contact killing experiment correlated with the survival rate on the antibacterial surfaces (compare Figure 1E). A constant increase in ion concentration was observed over time, with the highest copper levels detected after

om/doi/10.1002/admi.202500430 by Franca Arndt - Disch Zentrum F. Luft-U. Raum Fahrt In D. Helmholtz Gemein. , Wiley Online Library on [10/09/2025]. See the Terms and Conditions (https://onlinelibrary.wiley.

com/terms-and-conditions) on Wiley Online Library for rules of use; OA articles are governed by the applicable Creative Commons License

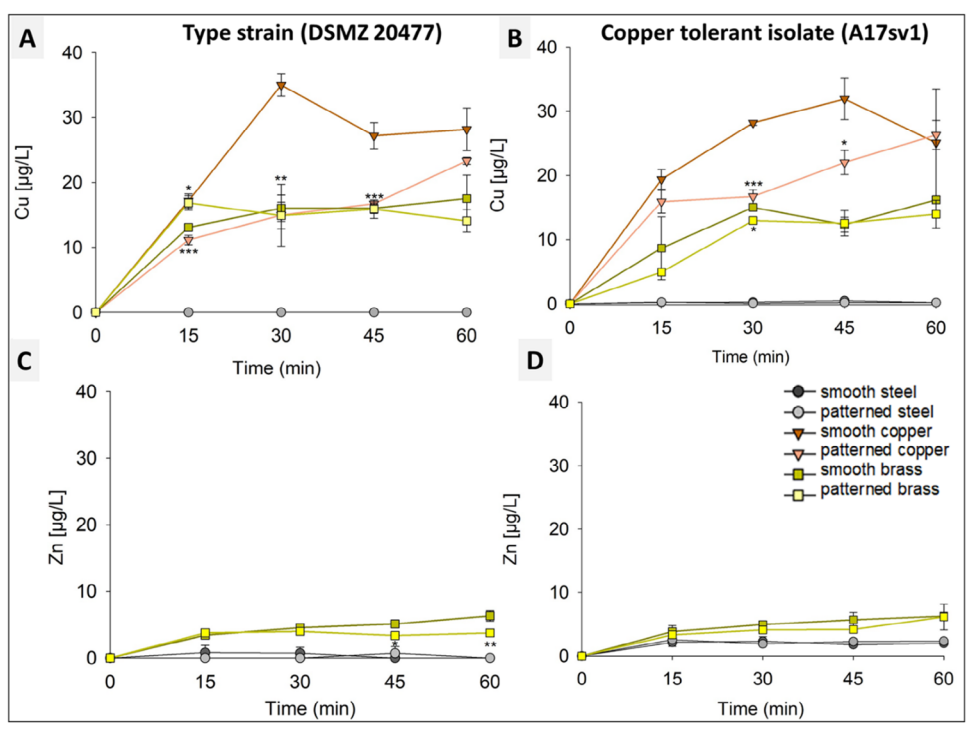


**Figure 2.** ICP-QQQ measurements of copper (Cu) and zinc (Zn) ion release in the cell suspension of *E. faecium* during contact to different metal surfaces for 15, 30, 45, and 60 min. **A)** Copper ion release from the type strain DSMZ 20477<sup>T</sup>, **B)** Copper ion release from the isolate A17sv1, **C)** Zinc ion release from the type strain DSMZ 20477<sup>T</sup>, **D)** Zinc ion release from the isolate A17sv1. Surface types: smooth steel, patterned steel (3 μm USP-DLIP), smooth copper, patterned copper (3 μm USP-DLIP), smooth brass, patterned brass (3 μm USP-DLIP). Measurements were performed in triplicate, and calculated error bars show the standard deviation of each sample (n = 3). Significance was determined by two-sample *t*-test; the conditions corresponding to the significance levels are as follows: \*p < 0.05, \*\*p < 0.01, \*\*\*p < 0.001.

60 min on patterned copper (26.3  $\mu g L^{-1}$ ) and smooth copper (25.0  $\mu g L^{-1}$ ). These findings align with the high antimicrobial effect of copper. Significant copper ion release from smooth copper was detected after 30 min and 45 min compared to the patterned surface (smooth copper/patterned copper: 30 min p < 0.001, 45 min p < 0.05, Figure 2B). Overall, the copper ion release from patterned copper surfaces increased steadily, whereas the smooth copper surfaces reached their peak concentration after 30 min (Figure 2A) and 45 min (Figure 2B). For the copper-tolerant strain (A17sv1), copper concentration on brass ranged from 4.70  $\mu g L^{-1}$  (brass) to 16.19  $\mu g L^{-1}$  (smooth). After 30 min, significantly lower zinc levels were found on smooth brass compared to patterned brass (p < 0.05, Figure 2B).

The zinc ion concentrations, measured in the cell suspension of the type strain (DSMZ 20477<sup>T</sup>) after 60 min of surface contact, ranged from 6.3  $\mu$ g L<sup>-1</sup> on smooth brass to 3.7  $\mu$ g L<sup>-1</sup> on patterned brass (Figure 2C). Significantly fewer ions were released from patterned brass at both 45 min and 60 min (smooth brass/patterned brass 45 min p < 0.05, 60 min p < 0.01). During the wet contact killing test with the two strains (DSMZ 20477 <sup>T</sup> and A17sv1), only relatively low concentrations of zinc were detected. The highest, nearly identical, were observed on the brass surfaces (smooth: 6.2  $\mu$ g L<sup>-1</sup> and patterned: 6.1  $\mu$ g L<sup>-1</sup>, Figure 2D).

A high ion release was expected from the roughened topography of the metal surfaces with a 3 µm structure, leading to increased ion release over time compared to smooth surfaces.<sup>[5]</sup>

However, the smooth metal surfaces showed the highest copper and zinc release. This effect was previously observed, however, only if ion release was tested without bacteria. Here, similar to our results, a peak was reached after 60 min, followed by a slight drop in ion concentration again. [6] The background of this phenomenon lies in the microstructural impact of USP-DLIP processing on both, the copper and the brass substrate, where corrosion resistance is enhanced due to superficial finegraining in copper<sup>[55]</sup> or dealloying in brass, leaving a decreased copper content and predominantly ZnO phase oxides close to the surface.<sup>[56]</sup> In both cases, copper ion release is decreased in a saline environment due to enhanced chemical surface passivation, which however, was found to be affected by the presence of bacteria due to a copper ion scavenging effect.<sup>[55]</sup> Copper scavenging is reported predominantly for Escherichia coli,[57] where a recent work involving USP-DLIP processed copper surfaces found a differing scavenging effect between gram-negative E. coli and gram-positive Staphylococcus aureus, pointing toward strain-specific bacteria/substrate interaction involved in antibacterial copper efficacy.[47] Compared to the very short time window of this study, a similar interaction can be observed, like for S. aureus in Müller et al. (2025), where both copper ion release and antibacterial activity levels are below the smooth reference within the initial time frame of exposure. After 60 min of exposure, both copper ion release and S. aureus deactivation are then peaking on USP-DLIP surfaces after enhanced bacterial cell damaging, which contributed to copper scavenging and hence ion

com/terms-and-conditions) on Wiley Online Library for rules of use; OA articles are governed by the applicable Creative Commons License

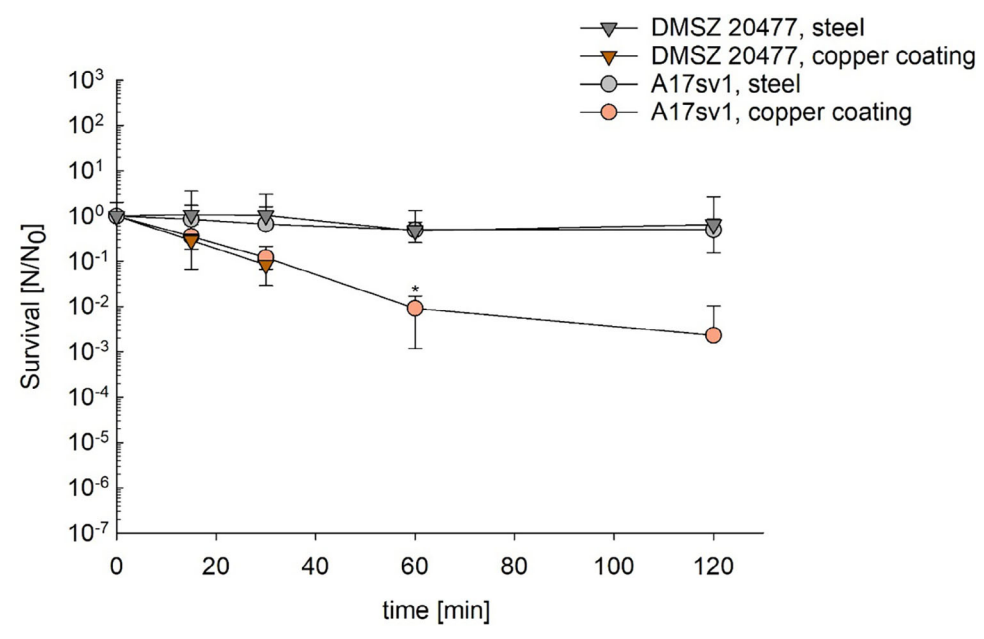


**Figure 3.** Survival data  $(N/N_0)$  of *E. faecium* (DSMZ 20477<sup>T</sup>, A17sv1) after contact to copper coatings for 15, 30, 60, and 120 min. (N number of surviving colony forming units (CFUs) at a given time point;  $N_0$  is the initial number of CFUs at the start of the experiment). Surface types: steel (reference material), copper coating. Measurements were performed in triplicate and the calculated error bars show the standard deviation of each sample (n = 3). Significance was determined by two-sample t-test; the conditions corresponding to the significance levels are as follows: p < 0.05.

release kinetics. In comparison, copper ion release similarly shows a peaking for the USP-DLIP processed copper surfaces with continuing exposure in this study, where however, the considerably lower number of seeded bacteria (10<sup>6</sup> vs 10<sup>9</sup> CFU mL<sup>-1</sup>) lead to a more rapid complete bacterial deactivation not enabling the measurement of a potential parallel increase of antibacterial efficacy of the USP-DLIP copper surfaces alongside further extending exposure. In another recent study by Timofeev et al. (2025), no significant difference in copper ion release between smooth and patterned copper, was observed in a study with A. niger, whereas antifungal properties have been improved by USP-DLIP.[20] This study reported even lower copper ion concentrations than those observed in our experiment, with less than 20 µg L<sup>-1</sup> copper ions measured from the same surfaces (smooth and 3 µm patterned copper).<sup>[20]</sup> In comparison to the pure copper surfaces, copper ion release on the brass samples remained at lower levels with the lowest values found on the USP-DLIP topography. This aligns with previous findings, where copper ion release is reduced after USP-DLIP treatment due to superficial alloy modification for the CuZn37 alloying type used.<sup>[56]</sup> In general, the zinc ion concentrations were relatively low compared to the copper ion release. This was expected since the brass surfaces contain 37% of zinc and 63% of copper. However, differences in the electrochemical behavior and dissolution kinetics of copper and zinc may also contribute to the distinct ion release profiles.

#### 2.3. Bacterial Survival on Antimicrobial Copper Coatings

Thin copper coatings offer various areas of application, such as hospitals, where antimicrobial coatings on frequently touched

surfaces can prevent the transmission of pathogens.<sup>[11]</sup> Instead of full copper materials, thin copper layers can be applied to different surfaces, while maintaining an antimicrobial effect

The surface and cross-sectional morphology of the sputtered copper coating were examined by scanning electron microscope (SEM), and its phase composition by X-ray diffraction (XRD). SEM of the polished, uncoated stainless steel shows scratches and isolated defects (Figure S4A, Supporting Information). After magnetron sputtering, the surface is uniformly covered by a dense, fine-grained copper layer with a compact, defect-free morphology (Figure S4B, Supporting Information). The cross-section shows a continuous ~1.5 µm film with columnar grains and a defect-free interface, indicating complete coverage (Figure S4C, Supporting Information). The XRD pattern exhibits the characteristic reflections of fcc Cu at  $2\theta \approx 43.3^{\circ}$  (111),  $50.4^{\circ}$  (200),  $74.1^{\circ}$ (220), and  $90.0^{\circ}$  (311), with a dominant (111) peak. No secondary phases of Cu oxides were detected, confirming the high purity and crystalline nature of the deposited coating (Figure S4D, Supporting Information).

Both the type strain (DSMZ 20477T) and the copper-tolerant strain (A17sv1) showed no reduction in survival after 60 min of exposure to the steel reference surface (**Figure 3**). However, no survival of the type strain after 15 min was detected on the copper coating, similar to the full copper material (Figure 1A). For the copper-tolerant isolate (A17sv1), a significant reduction in survival was observed after 60 min (p < 0.05, steel 60 min:  $4.97 \times 10^{-1}$ , copper 60 min:  $9.18 \times 10^{3}$ ), but still survived up to 120 min on the copper coating. Compared to the copper coating (2-log reduction; Figure 3), a more effective bacterial killing was observed on the copper material for the same isolate after 60 min (3-log reduction; Figure 1E). Therefore, while the

, Wiley Online Library on [10/09/2025]. See the Terms and Conditions (https://onlinelibrary.wiley.

s-and-conditions) on Wiley Online Library for rules of use; OA articles are governed by the applicable Creative Commons License

www.advmatinterfaces.de

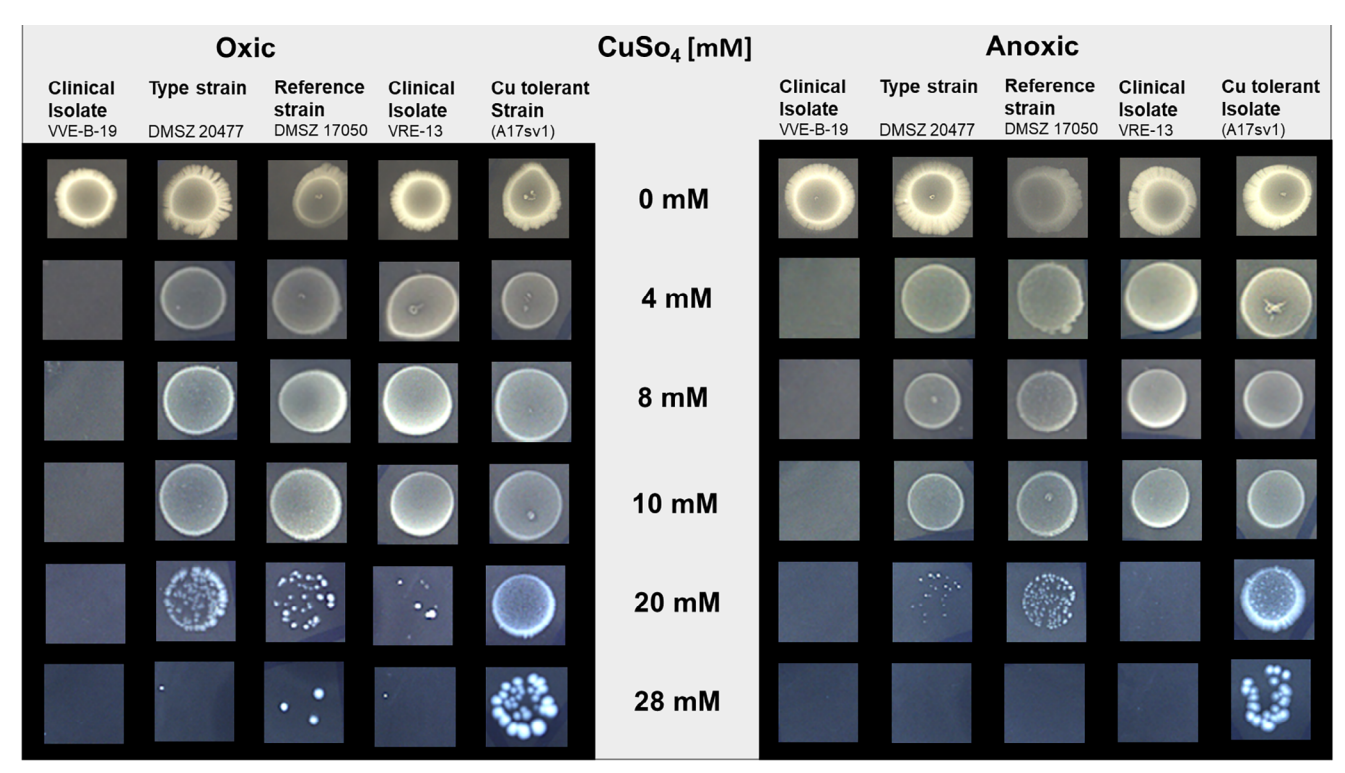


Figure 4. Minimal inhibitory concentration (MIC) of copper for *E. faecium* isolates (VVE-B-19, DSMZ 20477<sup>T</sup>, DSMZ 17050, VRE-13, A17sv1) after 7 days (at 37 °C) incubation on copper-infused BHI agar in different concentrations (0–28 mm CuSO<sub>4</sub>) under oxic conditions (left) and anoxic conditions (right). Initial cell concentration: 10 μL of 0.5 MFU (McFarland Unit). Original images of each colony on each plate are provided in the supplement (Figure S1, Supporting Information).

copper coating showed a similar antibacterial effect to the copper material against the type strain, the copper material was more effective against the copper-tolerant isolate A17sv1.

As described above, there is no doubt about the efficacy of copper coatings against pathogens, however, since antimicrobial coatings are a relatively new approach, the efficacy and longevity of coatings should be further investigated. [25,58] Because these factors can depend on hardness, adhesion strength, topography and wettability, and especially on the thickness of the coating, which influences the amount of copper ion release. [23,59,60] In our study, a thickness of  $\approx 1.5~\mu m$  of copper coatings was used (Figure S4, Supporting Information), which displayed antibacterial efficacy against *E. faecium*. Similarly, another study showed that even a thickness of 0.58  $\mu m$  can lead to a reduction in CFUs of different pathogens. [61]

# 2.4. MIC of Copper for E. faecium

Under both conditions, the minimal inhibitory concentration (MIC), Transmission Electron Microscopy (TEM) values ranged from 4 mm to >28 mm CuSO<sub>4</sub>. Without copper (0 mm), a distinct dendritic and/or branched colony morphology was observed after incubation in anoxic and oxic conditions for all five isolates. Interestingly, this morphology was not highly developed after incubation on the copper-infused agar. Up to 10 mm CuSO<sub>4</sub>, all five isolates displayed similar colony growth under both condi-

tions (anoxic/oxic conditions). The following results describe the data presented in **Figure 4**, from left to right. The clinical isolate (VVE-B-19) was only able to grow up to a concentration of 4 mm under both conditions (Figure 4). The type strain DSMZ 20477<sup>T</sup> and the reference strain DSMZ 17050 showed similar MIC values, with 28 mm under anoxic conditions and >28 mm under oxic conditions, indicating slightly increased copper tolerance in the absence of oxygen. Interestingly, the second clinical isolate (VRE-13), showed a much higher MIC to copper (oxic: >28 mm; anoxic: 20 mm) than the other clinical isolate (VVE-B-19). The greatest growth on high copper concentrations was exhibited the copper-tolerant isolate A17sv1. Independent of the incubation conditions, the isolate A17sv1 showed the most colonies with the MIC of > 28 mm (Figure 4).

Overall, the copper MIC values varied among the five *E. fae-cium* isolates, with higher MIC values observed under oxic conditions. Differences in growth between the two conditions became apparent, after exposure to 20 and 28 mm CuSO<sub>4</sub>. After incubation in 20 mm, all isolates showed single colony formation except for isolate A17sv1, which continued to form a single large colony.

As expected, the copper-tolerant isolate (A17sv1) showed tolerance to high copper concentrations, as it carries the *tcrB* gene, which confers copper resistance.<sup>[34,36]</sup> It was shown previously that isolates without this gene are able to tolerate copper concentrations up to 8 mm, however one clinical isolate we tested showed no growth on 4 mm CuSO<sub>4</sub> (Figure 4, VVE-B-19).<sup>[36]</sup> As indicated in previous research, the majority of environmental





www.advmatinterfaces.de

Enterococci, including animal and hospital isolates, have a MIC of 12 or 16 mm CuSO<sub>4</sub>. [62] Interestingly, the other *E. faecium* clinical isolate (VRE-13) had a MIC of over 28 mm under aerobic conditions and a MIC of 20 mm under anoxic conditions. For all isolates, it was noticeable that the yellow pigmentation decreased as the copper concentration in the agar increased, with all isolates appearing as white colonies at 28 mm. Literature shows that high pigmentation can be related to high environmental stress, like oxidative damage or UV-radiation. [63] It was also shown that, under aerobic conditions pigments can increase in Enterococci due to a higher environmental stress. [64] However, another study detected pigment loss in Pseudomonas under higher copper concentrations, which is in line with our findings. [65]

Enterococci are facultative anaerobic bacteria, meaning they are able to grow under both anoxic and oxic conditions. However, if there is more oxygen provided, this can result in upregulation of the glutathione metabolism, which then neutralizes ROS.[66] This could explain more growth under toxic conditions, even under copper stress. Furthermore, the observed effects under oxic conditions, showing more growth in high copper concentrations, may be influenced by the available oxygen. Under anoxic conditions, Cu2+ is reduced to Cu+ to enter the cell, which can be more toxic, due to its greater membrane permeability. [67-69] Another study showed a higher survival of Enterococcus under oxic conditions, which is in line with our results.<sup>[70]</sup> Moreover, the acquisition of the tcrYAZB operon provides Enterococcus isolates an advantage under anaerobic conditions in high copper concentrations. However, we observed a similar growth under oxic and anoxic conditions in 28 mm CuSO<sub>4</sub> (Figure 4).[70]

#### 2.5. MIC of Copper After Vancomycin Stress for E. faecium

The copper-tolerant isolate (A17sv1) showed a higher copper tolerance after exposure to high vancomycin concentrations. Here a correlation between a higher copper tolerance after prior vancomycin exposure is detectable. Without a prior vancomycin acclimatization, the strain grew at a maximum MIC of copper of 28 mм, (Figure 5). However, it increased after prior exposure to 10 mg  $L^{-1}$  vancomycin to a copper MIC of >30 mm. Interestingly, the copper-tolerant isolate (A17sv1) showed morphologically resembling small-colony variants (SCVs) under the highest copper CuSO<sub>4</sub> concentration tested (30 mm). This effect was not observed for the clinical isolates (VVE-B-19, VRE-13). Isolate VRE-13 showed the same copper MIC of 10 mm, regardless of vancomycin exposure or not. Similarly, the other clinical isolate (VVE-B-19) had a copper MIC of 4 mм (Figure 5) irrespective of the previous vancomycin concentrations it was exposed to.

The observed SCVs in the isolate A17sv1 suggest a potential link to increased copper tolerance. SCVs in Enterococci exhibit a thicker cell wall and a changed metabolism,<sup>[71]</sup> this could potentially lead to a higher copper tolerance, which could explain the SCVs under 30 mm of CuSO<sub>4</sub>. In contrast to that, SCVs of other species (*P. aeruginosa* and *S. aureus*) show a more susceptible phenotype to copper. This shows that the killing effect by copper is influenced by cell surface components, such as the overpro-

duction of extracellular polymeric substances in SCVs of *P. aeruginosa* and *S. aureus*. [72]

The correlation between an increased copper tolerance due to prior vancomycin exposure in the copper-tolerant isolate suggests a potential co-regulation of resistance genes, stress-induced efflux upregulation, or cell wall modifications, which could lead to the increased copper tolerance. However, this was only observed in the copper-tolerant isolate, not in clinical isolates (Figure 5). Hence, it might be deduced that this effect is specific for the tcrB gene and not the general copper response in Enterococci: The A17sv1 isolate harbors both the vancomycin and copper resistance gene, which are located on the same plasmid (Table 1).[34] Thus, a higher vancomycin exposure can lead to higher plasmid copper numbers, indirectly boosting tcrB expression, resulting in a higher copper tolerance. Additionally, a shared promoter could activate both operons (van operon, cop operon), suggesting co-resistance to vancomycin and copper when both operons are located on the same plasmid.[36] Importantly, this mechanism poses a great challenge to the intended use of copper surfaces: Antibiotic-resistant strains will have a selective advantage on copper surfaces, ultimately facilitating their spread. Hence, the exact mechanisms should be further explored before extensive usage of these surfaces. If the resistance genes for vancomycin and copper are not on the same plasmid, other global stress regulators like sigma factor B ( $\sigma^{B}$ ) could be triggered by the vancomycin stress, increasing the copper efflux pumps. However, this is highly unlikely, as other tested isolates lacking the trcB gene did not show increased copper tolerance after prior vancomycin exposure. Further experiments should reveal whether the high copper resistance induced by vancomycin, sustained or reversible.

# 2.6. SEM Analysis of E. faecium Isolates Cultivated in Liquid Medium With and Without Copper

As shown in **Figure 6**, the cells of *E. faecium* displayed a typical morphology of cocci, often organized in short chains or as diplococci. All isolates showed a rounder cell morphology after cultivation with copper. Additionally, for some cells, irregular cell proliferation and an uneven growth pattern were visible, especially for isolates A17sv1 and VVE-B-19. In general, cells without exposure to copper during incubation appeared less spherical (Figure 6). Some cells were larger and especially rounder for isolates cultivated in the presence of copper. Overall, all isolates (DSMZ 20477<sup>T</sup>, DSMZ 17050, A17sv1, VRE-13) except one (VVE-B-19), showed changes in their length and width if cultivated with copper. Three out of five isolates show a significant reduction in length if cultivated in copper, but not the coppertolerant isolate (A17sv1). Furthermore, all isolates showed a significant (p < 0.001) increase in width when cultivated in copper (Tables S2 and S3, Supporting Information). Furthermore, three out of the five isolates (DMSZ 20477T, A17sv1, VVE-B-19) showed evenly distributed external vesicles or extracellular polymeric substances on the cell surface (Figure 6-i,ii,iii). Those surface-associated structures were visible after both culture conditions, regardless if the cells were cultivated with or without copper. However, these structures did not appear uniformly on each cell. The type strain (DMSZ 20477<sup>T</sup>) cultured without copper

21967350, 0, Downloaded from https://advanced.onlinelibrary.wiley.com/doi/10.1002/admi.202500430 by Franca Andrt - Disch Zentrum F. Luft-U. Raum Fahrt In D. Helmholtz Gemein.

//onlinelibrary.wiley.com/terms-and-conditions) on Wiley Online Library for rules of use; OA articles are governed by the applicable Creative Commons License

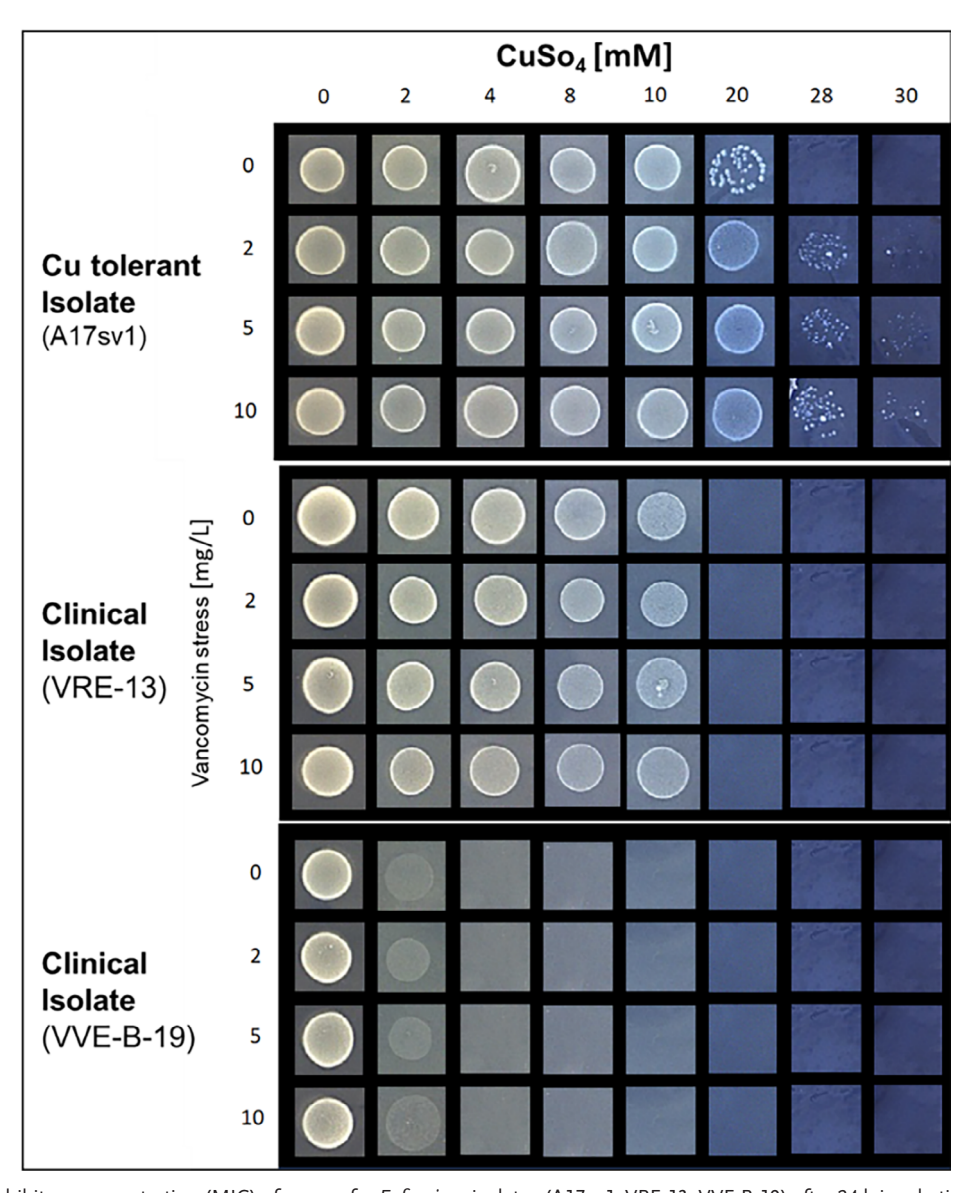


**Figure 5.** Minimal inhibitory concentration (MIC) of copper for *E. faecium* isolates (A17sv1, VRE-13, VVE-B-19) after 24 h incubation at 37 °C on CuSO<sub>4</sub>-infused BHI agar in different concentrations (0–30 mm CuSO<sub>4</sub>) following prior 72 h incubation at 37 °C on vancomycin-infused sheep blood agar with varying vancomycin concentrations (0–10 mg L<sup>-1</sup>). Initial cell concentration: 10  $\mu$ L of 0.5 MFU. Original images of each colony on each plate are provided in the supplement (Figure S2, Supporting Information).

**Table 1.** Comparative genomic table showing vancomycin (vanAB) and copper resistance genes (copAB, tcrB, cutC, cueO) and of five E. faecium isolates (DSMZ 20477<sup>T</sup>, DSMZ 17050, A17sv1, VRE-13, VVE-B-19).

	DSMZ 20477	DSMZ 17050	A17sv1	VRE-13	VVE-B-19	
Genes	Type strain	Reference strain	Animal isolate	Clinical isolate	Clinical isolate	
vanA	-	+	+	-	-	
vanB	-	-	-	+	+	
сорА	+	+	+	+	-	
сорВ	+	+	+	+	-	
tcrB	-	-	+	-	-	
cutC	+	+	+	+	+	
сиеО	-	-	+	-	-	

conditions) on Wiley Online Library for rules of use; OA articles are governed

Figure 6. SEM images of the five *E. faecium* isolates (type strain (DSMZ 20477<sup>T</sup>), reference strain (DSMZ 17050), copper-tolerant strain (A17sv1), clinical isolate (VRE-13), clinical isolate (VVE-B-19)) cultivated for 20 h at 37 °C without CuSO<sub>4</sub> (w/o CuSO<sub>4</sub>, left column) and with 2 mm CuSO<sub>4</sub> (+ CuSO<sub>4</sub>, right column). Surface-associated structures are marked with an arrow: i), ii), iii). See text for details. Scale bar: 400 nm.

exhibited those structures too, here the external substances seemed to connect two cells (Figure 6-i).

First, the observed morphological change to rounder cells could indicate a physiological adaptation to copper stress, potentially involving altered intracellular processes. It also may reflect a structural strategy to reduce the surface-area-to-volume ratio, thereby minimizing the exposure to toxic agents like copper.<sup>[73]</sup> Additionally, copper ions can disrupt cell envelope stability,<sup>[74]</sup> and their intake and accumulation may change the internal ion concentrations and osmotic balance, leading to an increased turgor pressure and rounder cells.

Secondly, the observed vesicles could be membrane vesicles, which may carry virulence factors, antimicrobial resistance determinants or play a role in intercellular communication trans-

ferring proteins, as previously shown by Wagner et al. (2018). <sup>[75]</sup> Alternatively, they may represent protein aggregation substances that provide better adherence and promote conjugative transfer of sex-pheromone plasmids. <sup>[76]</sup> Overall, these morphological changes already appeared after incubation in a low copper concentration of 2 mM CuSO<sub>4</sub>, suggesting that extreme stress is not required to induce alterations to the bacterial cells.

# 2.7. TEM Analysis of *E. faecium* Isolates Cultivated in Liquid Medium With and Without Copper

The morphological changes induced by treatment with 2 mm soluble copper (CuSO<sub>4</sub>) were the same in both strains investigated.

onlinelibrary, wiley, com/doi/10.0102/admi.202500430 by France Andri - Dsch Zentrum F. Luft-J. Raum Flart in D. Helmholtz Greenie, Wiley Online Library on [10/09/2025]. See the Terms and Conditions (https://onlinelibrary.wiley, converses-and-conditions) on Wiley Online Library for rule of use; OA articles are governed by the applicable Centwice Commons Licenses.

www.advancedsciencenews.com

www.advmatinterfaces.de

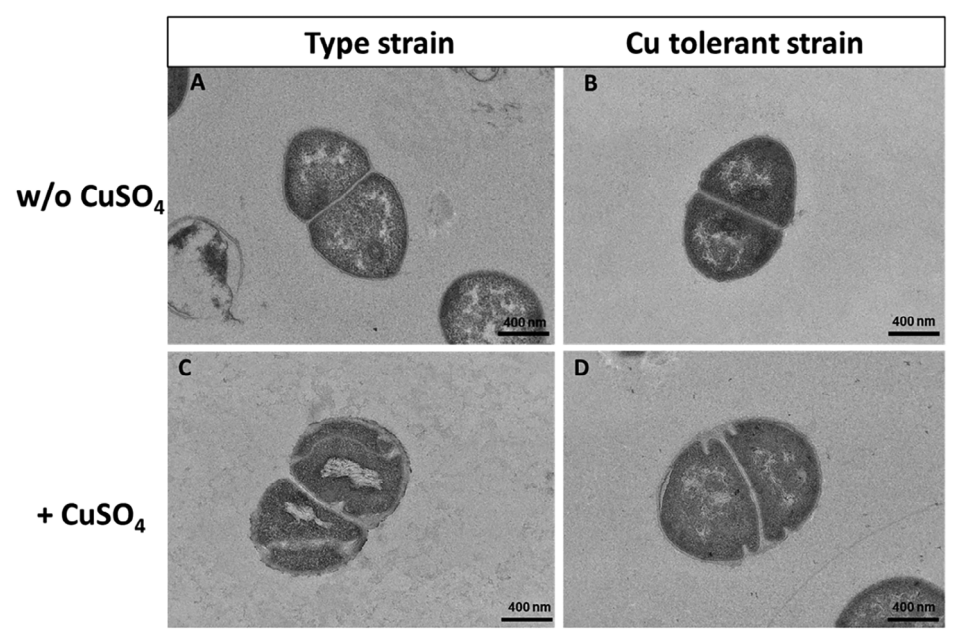


Figure 7. Transmission Electron Microscopy (TEM) images of *E. faecium* after 20 h of cultivation at 37 °C in BHI without and with 2 mm CuSO<sub>4</sub>. A)Type strain DSMZ 20477<sup>T</sup> without CuSO<sub>4</sub>, B) Copper-tolerant strain A17sv1 without CuSO<sub>4</sub>, C) Type strain DSMZ 20477<sup>T</sup> with 2 mm CuSO<sub>4</sub>, D) Copper-tolerant strain A17sv1 with 2 mm CuSO<sub>4</sub>. Scale bar: 400 nm.

Bacterial cell profiles appeared more spherical with a denser cytoplasm than in the untreated controls (Figure 7). The denser cytoplasm was frequently associated with a bundled fibrillar appearance of the bacterial nucleoid, which could be a consequence of the higher density of the cytoplasm, leading to a more ordered organization of the bacterial DNA.[77] Some copper-treated cells revealed slightly thickened cell walls in comparison to untreated cells. The most obvious difference between treated and untreated cell populations was the presence of extracted cells (not shown) and the frequent observation of additional cell division septa in treated cells (Figure 7C,D). The simultaneous formation of multiple septa could result from a stressed division process and may represent pseudo-multicellular bacteria, appearing larger with abnormally thick septal walls. Our size measurements by SEM support an increase in size. Cells with multiple division septa have been reported in a study after antibiotic treatments that inhibited cell separation.<sup>[78]</sup> Similarly, vancomycin exposure leads to a thicker cell wall, indicating a stress response. Thus, the formation of multiple division septa and the occasional thickening in response to copper and antibiotic stress reflect a shared stressadaptation mechanism that enhances cellular robustness.<sup>[79]</sup> Further experiments should analyze the molecular changes at the DNA and protein level to allow the generation of a mechanistic hypothesis. In this context, it would be very interesting to assess if and how the bacteria are re-adapting during growth in copperfree media after a former copper treatment.

## 2.8. Genomic Analysis of E. faecium Isolates

The results are compared in Table 1 with several genes related to vancomycin resistance (*vanAB*) and the copper homeostasis (*copAB*, *tcrB*, *cutC*). Overall, high-quality reads with most reads

above Q35 (Phred Score) were reached. The general length of genomic DNA for all isolates was between 2.591 and 3.285 kb. The two isolates, DSMZ 20477<sup>T</sup> and DSMZ 17050, carry the vanA gene, part of the vanA operon that confers resistance to the glycopeptide antibiotics vancomycin and teicoplanin.[80] The vanA nucleotide sequence from both isolates showed 100% identity (identical matches / aligned region length  $\times$  100) with vanA (Accession ID: UOA68407) when analyzed using BLASTn in the National Center for Biotechnology Information (NCBI) database. The clinical isolates VRE13 and VVE-B-19 harbor the *vanB* gene, which confers resistance to vancomycin (Table 1).[80] For both, a 96% identity was observed when compared to the vanB (Accession ID: WP\_002368691) in the NCBI database. Recently in Europe, a shift from vanA to vanB was observed in E. faecium, vanB, which is an inducible resistance mechanism activated by vancomycin exposure, poses challenges for detection and diagnostics. [81,82] The type strain (DSMZ 20477<sup>T</sup>), as to be expected, is vancomycin susceptible and does not carry a van gene (Table 1). Four out of five isolates (DSMZ 20477<sup>T</sup>, DSMZ 17050, A17sv1, VRE-13) carry the copA gene with a 99% identity to the sequence compared in NCBI (Accession ID: AQT55875). All isolates, except the clinical isolate VVE-B-19, carry the copAB genes for copper in- and efflux ATPases, which regulate the copper concentration during copper homeostasis in Enterococci (Table 1). The absence of copAB in VVE-B-19 corresponds with its copper-sensitive phenotype (Figure 4). The cop operon is essential in Enterococci for copper tolerance, its absence results in altered expression, leading to other regulatory mechanisms that maintain copper homeostasis, such as upregulation of sugar metabolism.[83]

In Enterococci *copA* encodes an ATPase essential in copper uptake, functioning as an influx pump.<sup>[37]</sup> The antagonist, ATPase *copB*, functions as an efflux pump transporting copper



**Table 2.** Comparative genomic table showing location of operons *co-pABYZ* and *vanA/vanB* in addition to the *tcrB* gene of five *E. faecium* isolates (DSMZ 20477<sup>T</sup>, DSMZ 17050, A17sv1, VRE-13, VVE-B-19). Closed genomes were obtained using Nanopore sequencing.

Isolates	Operon (van/cop)	Location
DSMZ 20477	cop operon	Chromosome
DSMZ 17050	vanA operon	Plasmid
	cop operon	Chromosome
A17sv1	vanA operon	Plasmid
	cop operon	Chromosome
	tcrB	Plasmid
VRE-13	vanB operon	Chromosome
	cop operon	
VVE-B-19	vanB operon	Chromosome
	cop operon	

out of the cell.<sup>[37]</sup> We observed 100% identity of *copB* (Accession ID: WP\_010776758) in the isolate A17sv1 and 99% identity for isolates DSMZ 20477<sup>T</sup>, DSMZ 17050, and VRE-13. As previously described,<sup>[34]</sup> and in line with our phenotypic data, the copper-tolerant isolate A17sv1 is the only among five isolates that carries the *trcB* gene with 100% identity to the *trcB* gene in the NCBI database (Accession ID: QJS01523). The *tcrB* gene has been detected in 15% of Enterococci isolates from various environments, with higher prevalence in *E. faecium* (23%) than in *E. faecalis*, and is associated with increased copper tolerance.<sup>[39]</sup>

All isolates (DSMZ 20477<sup>T</sup>, DSMZ 17050, A17sv1, VRE-13, VVE-B-19) carry the *cutC* gene, which encodes the copper homeostasis protein CutC, with 100% identity (Accession ID: WP\_002294560). It was shown that the expression of *cutC* is induced late during copper exposure and its absence leads to higher intracellular copper concentrations, suggesting an important role in copper efflux and homeostasis.<sup>[83]</sup> Additionally, *cueO* encoding for a multicopper oxidase, which oxidizes Cu(I) to Cu(II) might play a crucial role in detoxification and protection during copper stress.<sup>[84,85]</sup> The isolate A17sv1 shares 99% identity with the sequence from NCBI for *cueO* (Accession ID: ELA51234). None of the other *E. faecium* isolates carried *cueO*.

Further genome analysis revealed closed genomes with high coverage (see Table S1, Supporting Information) obtained through Oxford Nanopore sequencing. Table 2 compares the five isolates (DSMZ 20477T, DSMZ 17050, A17sv1, VRE-13, VVE-B-19). In all isolates, the *cop* operon was chromosomally encoded. Isolates associated with vanA resistance (DSMZ 17050, A17sv1) additionally carried a plasmid encoding these resistance genes (Table 2), which is in line with the literature. [86] Interestingly, in Germany, most E. faecium isolate harbor the vanB gene more frequently than vanA. All vanB-associated isolates (clinical isolates: VRE-13, VVE-B-19) showed a chromosomally encoded operon, which is most common for van B-type Enterococci.[87] As shown in Table 1, only A17sv1 harbors the plasmid-encoded tcrB gene, located on the same plasmid as vanA (Table 2) but not in close proximity. Both resistance genes are ≈47.000 bp apart (coding sequence (CDS) tcrB: 64,088-66,220 bp, CDS: vanA: 16,206-17,237 bp) and therefore co-regulation by the same promoter can be excluded.

# 2.9. Minimum Spanning Tree (MST) Analysis of Multilocus Sequence Typing (MLST) Data

**Figure 8A** presents a minimum spanning tree of the five isolates of this study (DSMZ 20477<sup>T</sup>, DSMZ 17050, A17sv1, VRE-13, VVE-B-19) grouped by sequence type (ST), and (B) a comparison to 1423 alleles of *E. faecium* isolates from different German cities, marked in red. The two clinical isolates VRE-13 and VVE-19 belong to ST117. The lineage of ST117 is hospital-associated and globally distributed, isolates of ST117 are often multidrugresistant and can cause severe infections.<sup>[88]</sup> DSMZ 20477<sup>T</sup> was assigned ST160, and DSMZ 17050 as ST25.

The isolate A17sv1 was identified as the ST6, the sequence type was found previously in *E. faecalis* of livestock (pig) origin.<sup>[89,90]</sup> However, MLST schemes are species-specific, so the same ST number does not indicate relatedness across species.

The different clusters show varying degrees of genetic distance (Figure 8B). The two clinical isolates VRE-13 and VVE-19, are isolated from Cologne and in close genetic relation/distance to many other *E. faecium* isolates. This could indicate a hospital outbreak of one clonal lineage. However, DSMZ 17050 has a long and separate branch, which indicates a high genetic difference compared to the other isolates. However, DSMZ 17050 has a long and separate branch, which indicates a high genetic difference compared to the other isolates. Here, a difference of 909 alleles was observed between DSMZ 17050 and an isolate from Cologne, indicating that these isolates are genetically distinct. The type strain DSMZ 20477<sup>T</sup> differs by 554 alleles from the same Cologne isolate. It shares a branch with the animal-derived isolate A17sv1, but still exhibits a difference of 969 alleles.

#### 3. Conclusion

In this study, we investigated the copper resistance of five E. faecium strains with varying pheno- and genotypes. We showed that each isolate responded differently to varying copper concentrations and surface types. In general, full copper materials were more effective than coatings, while the topography (3 µm USP-DLIP) did not affect bacterial survival significantly. These results and their difference to previous studies conducted with E. coli<sup>[6]</sup> may be attributed to not only the different cellular construction (Gram-negative vs. Gram-positive) but also to variations in cell size and shape. Ongoing research already focuses on the response of bacterial communities to surfaces with different copper concentrations.[91] Future studies should prioritize those by exploring a broader range of surface topographies to optimize antimicrobial effectiveness. In addition, maximum intracellular copper concentrations and their relation to higher copper tolerance should be investigated. This should be combined with transcriptomic data, simultaneously allowing assessment of gene expression changes under copper stress. Proteomic analysis would provide deeper insight into functionally relevant pathways like oxidative stress responses, copper homeostasis, and efflux systems, which contribute to copper tolerance.

A pivotal aspect of our study was an increase in the copper MIC following prior vancomycin exposure in the copper-tolerant isolates, which harbors the *tcrB* gene, but not in the clinical isolates. In the future, where a rise in copper and antibiotic resistance in bacteria can be expected<sup>[92,93]</sup> this result should be taken very

21967350, 0, Downloaded from https://advanced.onlinelibrary.wiley.com/doi/10.1002/admi.202500430 by Franca Arndt - Disch Zentrum F. Luft-U. Raum

, Wiley Online Library on [10/09/2025]. See the Terms and Conditions (https:

and-conditions) on Wiley Online Library for rules of use; OA articles are governed by the applicable Creative Commons License

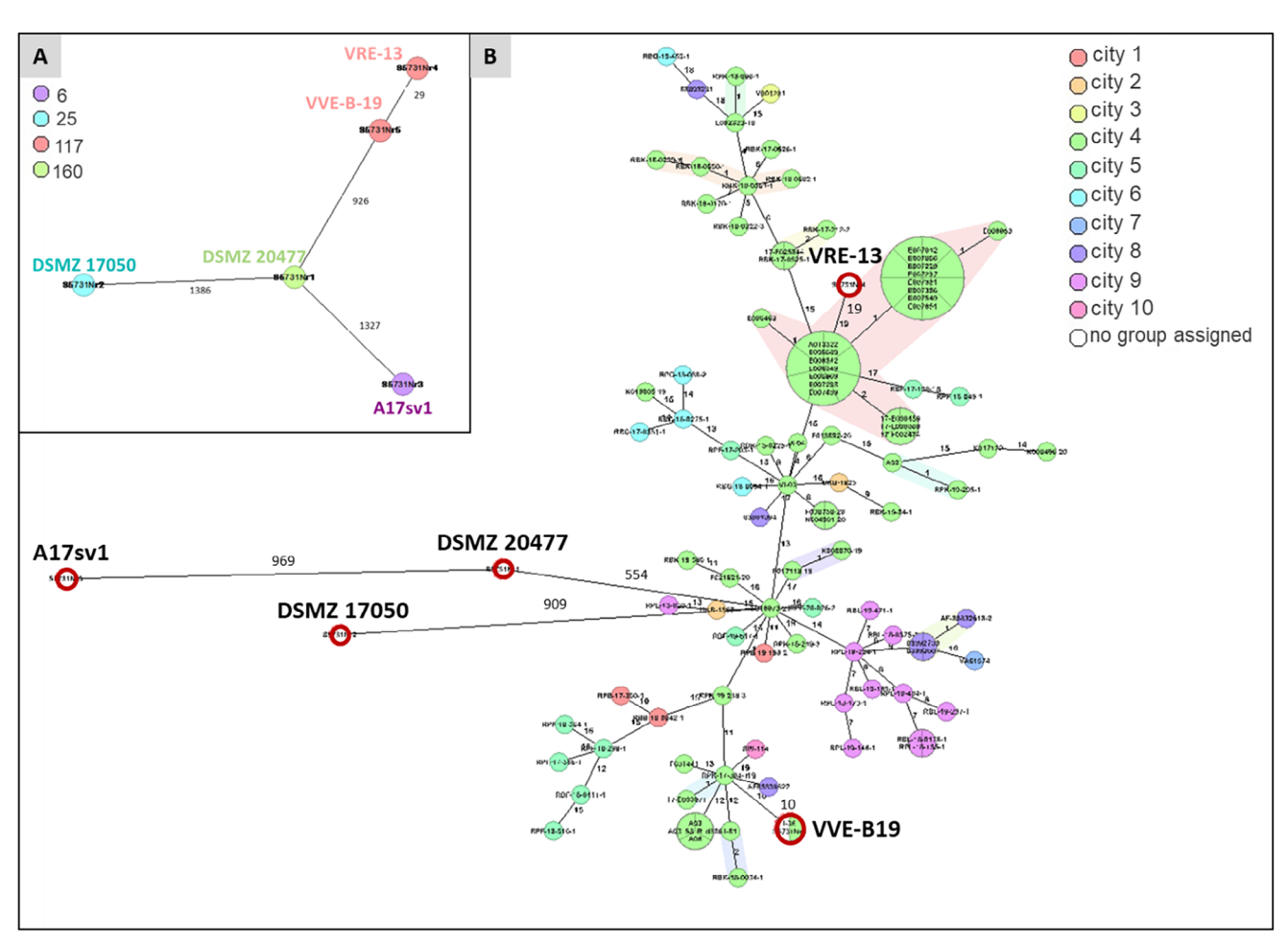


**Figure 8.** A) Minimum spanning tree of five *E. faecium* isolates (DSMZ 20477<sup>T</sup>, DSMZ 17050, A17sv1, VRE-13, VE-B-19) grouped by sequence type (ST). B) Minimum spanning tree of five *E. faecium* isolates (DSMZ 20477<sup>T</sup>, DSMZ 17050, A17sv1, VRE-13, VVE-B-19) compared to 1423 other *E. faecium* alleles from different German cities. Five *E. faecium* isolates investigated in this study are marked red (DSMZ 20477<sup>T</sup>, DSMZ 17050, A17sv1, VRE-13, VVE-B-19). Program: Ridom SeqSphere+ with a MST cluster distance threshold 3.

seriously, especially regarding the application of antimicrobial copper surfaces in hospitals. Here, monitoring should be mandatory if such surfaces are implemented, for the development of copper tolerance and antibiotic resistance in hospitals.

In summary, for effective and safe usage of antimicrobial surfaces in clinical environments, optimizing their topography and further enhancing our knowledge of antibiotic-metal coresistances is imperative.

#### 4. Experimental Section

Functionalized Metal Materials: The three investigated materials oxygen-free Cu (>99.95%), M37 brass (Cu 63%, Zn 37%) (Wieland), and AISI 304 stainless steel (Brio) were purchased as 1 mm metal sheets. Sampling was done by sectioning into metal plates of  $10 \times 25 \text{ mm}^2$ . The stainless-steel samples already exhibited a mirror-polished surface finish, whereas both Cu and brass underwent a multi-step polishing process on an automated TegraPol-21 system (Struers, Ballerup, Denmark) to receive a similar surface finish. Shares of the polished samples were used as topographically smooth references.

The mirror-polished metal samples were laser processed by a laser interference setup that has previously been described in Müller et al.

2020 (schematically illustrated in **Figure 9**).<sup>[40]</sup> The setup comprises a Ti:Sapphire laser source (Solstice ACE, Spectra Physics) that emits ultrashort laser pulses at a pulse duration of tp = 150 fs (Full Width at Half Maximum, FWHM), a centered wavelength  $\lambda$  of 800 nm, and 1–5 kHz pulse frequency, and an optical USP-DLIP setup for two-beam laser interference. Within the optical setup an aperture and  $\lambda$ /2 wavelate are used modulate both spot geometry and linear beam polarization. A diffractive optical element (DOE) generates two partial beams that are both overlapped and focused on the sample surface by a lens system. Analogous to the Fresnel mirror test setup, the generated pattern periodicity P is modulated by the relation between the laser wavelength  $\lambda$  and the angle of incidence  $\theta$  presented in Eq. (1):

$$P = \frac{\lambda}{2 \tan(\theta)} \tag{1}$$

For the pattern periodicity of 3  $\mu m$  used in this work,  $\theta$  was set to 7.66°. Patterning of the sample surfaces was conducted at 1 kHz pulse frequency and a fluence of either 2.1 J cm<sup>-2</sup> (Cu and stainless steel) or 0.98 J cm<sup>-2</sup> (brass), and a pulse overlap of N = 10 for 3  $\mu m$  pattern scale. The USP-DLIP processed Cu and brass samples underwent immersion etching in citric acid in an ultrasonic bath (1 min in 3% citric acid for Cu and 2 min in 5% citric acid for brass). Citric acid treatment was applied to minimize the influence of laser-induced chemical modifications, such

21967350, 0, Downloaded from https://advanced.onlinelibrary.wiley.com/doi/10.1002/admi.202500430 by Franca Arndt - Disch Zentrum F. Luft-U. Raum Fahrt in D. Helmholtz Gemein.

, Wiley Online Library on [10/09/2025]. See the Terms and Conditions (https://onlinelibrary.wiley.

com/terms-and-conditions) on Wiley Online Library for rules of use; OA articles are governed by the applicable Creative Commons License

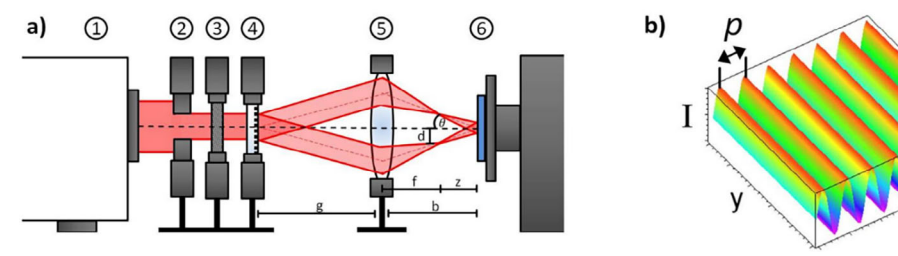


Figure 9. a) The optical setup applied for USP-DLIP consisting of 1 laser source, 2 aperture, 3 wave plate, 4 DOE, 5 lens system, 6 automated two axes (x,y) sample mount. b) the 1D sinusoidal intensity pattern induced by two-beam interference. The periodicity P accounts for the distance between two intensity maxima or minima. Reproduced with permission from Müller et al.<sup>[40]</sup>. Copyright 2020, Springer. The figure was also included in Timofeev et al. (2025) [20]

as surface oxides, thereby isolating the effect of surface topography on microbial inactivation. This approach reduces experimental variability and enables a more targeted investigation of topography-driven antimicrobial performance.[6,41,56,94,95]

The USP-DLIP-induced topography was characterized via confocal laser scanning microscopy (LSM) (LEXT OLS4100 3D Measuring Laser Microscope by Olympus applying the  $50\times$  lens, 2x and 6x digitally increased magnification at a laser wavelength 405 nm).

The surface roughness characteristics of both the polished and laser-structured samples in this study are consistent with those reported in previous works using identical preparation parameters. [41,94,96] Overall, laser-structured surfaces produced using ultrashort pulsed irradiation are known to exhibit a transient wettability behavior, initially displaying hydrophilicity that gradually shifts to a stable hydrophobic state within approximately three weeks post-processing. [41,56,60,94] All used surfaces are listed in **Table 3**.

Magnetron Sputtering: The substrate material used was  $1\times1$  cm V2A steel. The samples were ground to 4000 grit on one side to prepare the coating. The coating was then deposited using a batch magnetron sputtering system (Z400, Systec SVS vacuum coatings, Karlstadt, Germany). Before deposition, the ground side of the steel sample was subjected to Ar+ ion etching to clean and activate the sample surface. Dense polycrystalline Cu targets with a diameter of 100 mm were used as the target material. A power of 300 W was applied to the Cu target with a deposition time of 12 min. The total pressure during deposition was about 0.78 Pa in an Ar (Argon) atmosphere with a constant flow rate of 20 sccm.

The sputtered coatings were analyzed by X-ray diffraction (Bruker D8 Advance, Cu K $\alpha$  radiation, EVA/Topas 4.2 software package, Bruker AXS, Karlsruhe, Germany) (Figure S4D, Supporting Information). The deposited coatings are crystalline, which resulted from X-ray diffraction measurements. To determine the thickness of the coatings, cross-sections were analyzed using a scanning electron microscope (SEM) (DSMZ Ultra 55, Carl Zeiss NTS, Wetzlar, Germany at a voltage of 2 kV (Figure S4 C, Supporting Information). The coatings resulted in a thickness of  $\approx$ 1.5  $\mu$ m.

**Table 3.** List of all used metal surfaces in the "Wet-Contact Killing" experiment. USP-DLIP: ultrashort pulsed direct laser interference patterning. Materials used: smooth steel, steel modified with a 3  $\mu$ m USP-DLIP pattern, smooth copper, copper modified with a 3  $\mu$ m USP-DLIP pattern, smooth brass, brass modified with a 3  $\mu$ m USP-DLIP pattern.

Material	USP-DLIP	Specification	Manufacturer	
Steel	/	AISI 304 stainless steel	Brio	
Steel	3 μm	AISI 304 stainless steel	Brio	
Copper	/	OF-CU	Wieland	
Copper	3 μm	OF-CU	Wieland	
Brass	/	CuZn37	Wieland	
Brass	3 μm	CuZn37	Wieland	

Top view imaging was performed on both the uncoated stainless steel and the copper-coated stainless steel by using the SE detector at a voltage of 5 kV (Figure S4A,B, Supporting Information).

Antibacterial Tests—Cultivation of E. faecium Isolates: In this study, five E. faecium isolates were tested, including the type strain DSMZ 20477<sup>T</sup> (ATCC 19434, (Orla-Jensen 1919; Schleifer and Kilpper-Bälz 1984) and a reference strain DSMZ 17050 (Orla-Jensen 1919; Schleifer and Kilpper-Bälz 1984), ordered from the DSMZ-German Collection of Microorganisms and Cell Cultures GmbH. These standardized strains were chosen to enable reproducibility and comparability across studies. Additionally, two clinical isolates (VVE-B-19 and VRE-13) from the University Hospital of Cologne were obtained from different clinical specimens, which were prior investigated by Arndt et al.[97] These represent humanassociated, hospital-relevant isolates and reflect the challenges of nosocomial infections. Furthermore, one copper-tolerant E. faecium isolate (A17sv1; Pasteur Institute CIP 106701) from the livestock-associated clade was included as a representative of a strain with known copper tolerance, to gain insights into how such phenotypes may influence survival on copper surfaces. All isolates were selected based on differences in their vancomycin resistance. Thus, vancomycin-resistant Enterococci (VRE) (DSMZ 17050, VRE-13, A17sv1), vancomycin-susceptible Enterococci (VSE) (DSMZ 20477<sup>T</sup>), and vancomycin variable Enterococci (VVE) (VVE-B-19) were included. [98]

All isolates were additionally selected based on differences in their vancomycin resistance profiles. Hence, vancomycin-resistant Enterococci (VRE: DSMZ 17050, VRE-13, A17sv1), vancomycin-susceptible Enterococci (VSE: DSMZ 20477<sup>T</sup>), and vancomycin-variable Enterococci (VVE: VVE-B-19) were included, ensuring a broad spectrum of resistance phenotypes and environmental backgrounds.

For cultivation all *E. faecium* isolates, stored as cryocultures ( $-80\,^{\circ}$ C), were plated on sheep blood agar (SBA; OxoidTM, Thermo Fisher Scientific Inc., Waltham, USA) and incubated for 24 h at 37 °C (Incubator Heraeus INSTRUMENTS, Germany). Colonies from the 24 h plates were picked to prepare a 20 mL liquid culture in Brain Heart Infusion (BHI), which was incubated in a shaking incubator at 180 rpm at 37 °C for 24 h. Subsequently, 2 mL of the cell suspension was centrifuged for 5 min at 13,000 × g and washed three times with Phosphate Buffered Saline (PBS). A McFarland standard of 0.83 MFU was set using a nephelometer (DensiCHE, bioMérieux Inc., USA). Afterward the cell suspension was diluted 1:100 to reach an initial average cell count of  $1.5 \times 10^6$  CFU mL $^{-1}$ , from which 40 µL were taken, resulting in an initial cell number of  $6.0 \times 10^4$  CFU. With this cell count applied to each 40 µL droplet on a contact surface with a 6 mm diameter, a monolayer is formed with a coverage ranging from 93.4% to 98.9%, with a presumed cell size of 1 µm.

An overview of the experimental design, including which specific *E. fae-cium* isolates were used in each assay, is provided in **Table 4**.

Wet-Contact Killing Assay: The wet-contact killing experiment evaluated bacterial survival after exposure to smooth metal materials (copper, brass) and 3  $\mu m$  USP-DLIP modified surfaces (patterned copper, patterned brass) to determine the antimicrobial effect of each material. Smooth steel and 3  $\mu m$  USP-DLIP modified steel were used as reference materials. Comparisons were made between copper/brass and steel to evaluate



www.advmatinterfaces.de

**Table 4.** Overview of Experiments, highlighting the use of *E. faecium* isolates in each experiment (Type strain DSMZ 20477<sup>T</sup>, Reference strain DSMZ 17050, Clinical isolate VRE-13, Clinical isolate VVE-B-19, Copper-tolerant isolate A17sv1). The table summarizes the main experiments, divided into antibacterial tests, analysis of morphological effects of soluble copper, and genomic investigations.

Experiment	Isolates					
	DSMZ 20477 <sup>T</sup> Type strain	DSMZ 17050 Reference strain	VRE-13 Clinical isolate	VVE-B-19 Clinical isolate	A17sv1 Cu tolerant isolate	
Antibacterial Tests						
Bacterial Survival on Functionalized Surfaces	Х	Х	X	Х	Х	
Cu and Zn Ions Release Rate Measurement	X				Х	
Bacterial Survival on Antimicrobial Copper Coatings	Χ				Х	
MIC of Copper	X	X	X	X	X	
MIC of Copper after Vancomycin Stress	X		X	X		
Morphological Effects of Soluble Coppe	er					
Scanning Electron Microscopy	X	Х	X	Х	Х	
Transmission Electron Microscopy	X	X				
Genomic Analysis						
Illumina Sequencing	X	Х	X	Х	X	
Nanopore Sequencing	X	X	X	Х	X	
Minimum Spanning Tree Analyses	X	X	X	Χ	Х	

antibacterial and material-specific effects and between smooth and patterned surfaces to assess topography effects.

Additionally, the antimicrobial efficiency of copper coatings, consisting of a copper layer on steel applied via magnetron sputtering, was tested in a preliminary experiment using two E. faecium isolates (DSMZ 20477<sup>T</sup>, A17sv1). The initial starting cell number for all experiments ranged from 10<sup>5</sup> to 10<sup>6</sup> colony-forming units per milliliter (CFU/mL). The experiment was performed with five isolates: (DSMZ 20477T, DSMZ 17050, A17sv1, VRE-13, VVE-B-19 and all measurements were performed in triplicates, the calculated error bars show the standard deviation of each sample (n = 3)(Figure 1). To ensure consistent and comparable results, all E. faecium isolates were tested under identical experimental conditions on the functionalized surfaces. The steel, used as a reference material, was sterilized by autoclaving, while the copper and brass (CuZn37: 63% copper, 37% zinc) materials and the coatings were disinfected with ≥99,5% ethanol (ROTH, Karlsruhe, Germany) before use in the experiment. After the polyvinyl chloride film/tape (PVC) (Professional Grade super 33+, Scotch, Germany) was cut according to the size of the materials ( $10 \times 25$  mm) it was punched three times and applied to the materials. Here, the punched holes on one surface provide three 6 mm diameter areas for the contact of the cell suspension with each surface. After application of the tape to all materials, they were sterilized under UV-light for 30 min. To ensure stable humidity and to avoid evaporation during the experiment, a wet soft tissue was placed next to the surfaces in a closed sterile petri dish (SARSTEDT, Germany). Then, 40 µL of the bacterial suspension, prepared as described (4.3.1 Cultivation of E. faecium isolates), was applied to each surface. After incubation at room temperature for 0, 15, 30, 45, and 60 min.,  $10\,\mu L$  of the cell suspension was carefully resuspended and transferred to 90  $\mu L$  of phosphate buffered saline (PBS) in a tissue culture plate (96 well plate, flatbottom, polystyrene, TPP, MERK, Germany). Temperature and relative humidity (RH) were monitored during the whole experiment with a thermohygrometer (TFA Dostmann, Germany) and averaged 21  $^{\circ}\text{C}$  and 44 % RH during the experiments. To analyze the number of colony-forming units per milliliter (CFU/mL), a serial dilution of the cell suspension in PBS was

prepared. Subsequently, 25  $\mu$ L of each dilution step was plated on sheep blood agar (SBA; OxoidTM, Thermo Fisher Scientific Inc., Waltham, USA) and incubated at 37 °C for 24 h (Incubator Heraeus INSTRUMENTS, Germany). The survival after contact to each surface was calculated using the formula N/N<sub>0</sub>, N<sub>0</sub> the initial number of CFUs at the start of the experiment is divided by N, the number of surviving CFUs at a given time point.

Cu and Zn Ions Release Rate: During the wet-contact killing experiment, the majority of bacterial cells are sedimenting within  $\approx\!20$  min on each metal surface, providing direct cell-surface interactions. Although direct surface contact was shown to promote the active antimicrobial effect,  $^{[99]}$  the quantitative release of metal ions into the liquid remains as the predominant driving force behind bactericidal activity. To gain deeper insights into the actual concentrations of metal ions surrounding the cells during surface contact, copper and zinc ion release was measured at each time point using inductively coupled plasma triple quadrupole mass spectrometry (ICP-QQQ) for two isolates: the type strain DSMZ 20277 and the copper-tolerant isolate A17sv1.

A 13 mL screw cap tube (101  $\times$  16.5 mm, PP 1, Sarstedt, Germany) was prepared with 3995  $\mu L$  of 0.69% nitric acid. Then 5  $\mu L$  of cell suspension was taken from the different surfaces after each time point (0, 30, 45, 60 min) after the wet-contact killing assay (4.3.2). Three replicates were taken from each surface.

To determine the Cu and Zn content, the solutions were diluted by a factor of 3 and measured with an Inductively Coupled Plasma Triple Quadrupole Mass Spectrometry (Agilent 8900 ICP-QQQ, Agilent Technologies). Ultrapure water with a resistivity of 18.2 M $\Omega$ cm (0.055  $\mu$ S cm $^{-1}$ ) from a PURELAB Chorus 1 ultrapure water filtration system (Elga Lab-Water) was used for dilution, and HNO $_3$  (ROTIPURAN Supra 69%, Carl Roth) for acidification of all measurement solutions. A solution containing 10 mg L $^{-1}$  each of Sc (1.0 g L $^{-1}$  in 5% HNO $_3$ , Alfa), Y (1.0 g L $^{-1}$  in 2%–3% HNO $_3$ , Merck Certipur) and Ho (1.0 g L $^{-1}$  in 2%–3% HNO $_3$ , Merck Certipur) in ultrapure water was prepared as an internal standard solution for all ICP-QQQ measurements. Argon 5.0 (Ar  $\geq$  99.999 mol%, ALPHAGAZ 1 Argon, Air Liquide) was used as plasma gas. For quantification purposes,

**ADVANCED** SCIENCE NEWS

www.advancedsciencenews.com



www.advmatinterfaces.de

an external calibration was prepared using Cu (1.0 g  $L^{-1}$  in 0.5 mol  $L^{-1}$  HNO<sub>3</sub>, Merck Certipur) and Zn (1.0 g  $L^{-1}$  in 0.5 mol  $L^{-1}$  HNO<sub>3</sub>, Merck Certipur) ICP-MS standard solutions. The measurement of  $^{63}$ Cu,  $^{64}$ Zn,  $^{65}$ Cu, and  $^{66}$ Zn was then performed in He collision gas mode.

Copper MIC: To gain more insights into the copper tolerance of the five *E. faecium* isolates (DSMZ 20477<sup>T</sup>, DSMZ 17050, VRE-13, VVE-B-19, A17sv1), as a preliminary experiment, the MIC of copper was determined using copper-infused brain heart infusion (BHI) agar in the range of 0 to 28 mm  $CuSO_4$ . Since *E. faecium* is a facultative anaerobic, the MIC of copper was tested under both anoxic and oxic conditions.

To determine the MIC of copper for each of the five *E. faecium* isolates, fresh overnight colonies were picked to prepare 0.5 MFU and 10  $\mu L$  were pipetted on the copper-infused agar. To prepare the copper-infused agar, 40 mm of CuSO4 stock solution was poured into a petri dish and was gently mixed with Brain Heart Infusion Agar (Becton, Dickinson and Company, USA) to reach concentrations of: 0, 4, 8, 10, 20, and 28 mm. To achieve a solid medium even at higher copper concentrations, the double amount of agar (32 g L $^{-1}$ ) as recommended by the manufacturer was added. After 7 days of incubation at 37 °C, colony growth was assessed for each concentration (0–28 mm CuSO4). For growth under anoxic conditions, plates were incubated in GENbag anaer plastic bags (GENbag anaer, bioMérieux Inc., USA).

MIC of Copper After Vancomycin Stress: To deepen the understanding of interactions between different stressors, such as antibiotics and copper, and to reveal potential cross-tolerance, three E. faecium isolates (VVE-B-19, VRE-13, A17sv1) were investigated. The isolates were first exposed for 72 h at 37 °C to vancomycin-infused sheep blood agar (SBA; OxoidTM, Thermo Fisher Scientific Inc., Waltham, USA) at concentrations of 2, 5, and 10 mg L $^{-1}$ , and were subsequently tested for their MIC to copper. For this, all isolates were inoculated daily (in total 3 days) on a new sheep blood agar plate with the same vancomycin concentration. Subsequently, a 0.5 MFU standard was prepared and 5  $\mu$ L were plated on copper-infused agar with different concentrations (2, 4, 8, 10, 20, 28, 30 mm CuSO $_4$ ). After incubation for 24 h at 37 °C, the growth of the E. faecium isolates on the copper-infused agar was assessed.

Morphological Effects of Soluble Copper on E. faecium—Scanning Electron Microscopy (SEM): For analyzing the phenotypic changes of E. faecium cultivated in soluble copper-containing media, five isolates (DSMZ 20477<sup>T</sup>, DSMZ 17050, A17sv1, VRE-13, VVE-B-19) were compared by scanning electron microscopy (SEM). It was previously described by Hasman and Aarestrup (2002) that copper resistance in E. faecium could be induced by being exposed to low concentrations of copper.<sup>[34]</sup> Thus, the isolates were cultivated in BHI media with and without 2 mm CuSO<sub>4</sub> for 20 h to investigate the impact of copper on the bacterial cell morphology and copper-induced physical damage or adaptive features.

The bacterial suspension was prepared in a tissue culture plate (24) well plate, flat bottom, polystyrene, TPP, MERK, Germany) with 50 μL E. faecium glycerol stock, 1235 μL tryptic soy broth (TSB), and 214.28 μL phosphate-buffered saline (PBS). For bacteria cultured in copper, instead of PBS, 214.28 µL of 28 mm CuSO<sub>4</sub>·5 H<sub>2</sub>O stock solution was added to reach a final concentration of 2 mM CuSO<sub>4</sub>·5 H<sub>2</sub>O (Copper (II)-sulfate pentahydrate, MERK, Germany). The tissue culture plate was incubated for 20 h at 37 °C in an incubator (Incubator Heraeus INSTRUMENTS, Germany). To recover the cells, the suspension was transferred into 1.5 mL reaction tubes (SARSTEDT, Germany) and centrifuged at 3000 × g for 5 min using a centrifuge (Heraeus pico 21, Thermo Fisher Scientific Inc., Waltham, USA). All samples were fixed in a solution of 1% paraformaldehyde, 2.5% glutaraldehyde in 50 mm HEPES buffer for 24 h. Subsequently, 70 μL of a 1% Aclian blue solution was spotted on 12 mm glass coverslips for 30 min to adsorb the suspended bacteria to the now charged surface. After the Alcian blue was removed by dip-washing in ddH2O, 70 µL of the respective samples were spotted on the coverslips and incubated for 30 min. All samples were washed in 50 mm HEPES, dehydrated in 30%, 50%, 70%, 90%, 95%, 100% ethanol, dried overnight in hexamethyldisilazane, mounted on aluminum stubs, sputter coated with an 8 nm layer of gold-palladium and finally examined in the SEM (Zeiss 1530 Gemini, Carl Zeiss Microscopy) operating at 3 kV using the in-lens secondary electron detector.

The length and width were quantified for 15 cells per condition/strain. Measurements were done manually using ImageJ (ImageJ-win64) from 3 cells per image across 5 SEM images. Statistical comparisons were determined by two-sample t-test (n = 15).

Transmission Electron Microscopy (TEM) of Thin Sections: To deepen the understanding of how copper may impact internal structures, molecular interactions and physiology a TEM analysis of thin sections through the type strain (DSMZ 20477<sup>T</sup>) and copper-tolerant *E. faecium* strain (A17sv1) was performed.

To assess the phenotype of *E. faecium* cultivated with copper (50  $\mu$ L *E. faecium* glycerol stock, 1235  $\mu$ L tryptic soy broth (TSB), and 214.28  $\mu$ L of 28 mm CuSO<sub>4</sub>·5 H<sub>2</sub>O stock solution) and without copper (50  $\mu$ L *E. faecium* glycerol stock, 1235  $\mu$ L tryptic soy broth (TSB), and 214.28  $\mu$ L phosphate buffered saline (PBS)) the bacterial suspension was prepared in a tissue culture plate (24 well plate, flat bottom, polystyrene, TPP, MERK, Germany). The final concentration of the cell suspension with copper was 2 mm CuSO<sub>4</sub>·5 H<sub>2</sub>O (Copper (II)-sulfate pentahydrate, MERK, Germany). The tissue culture plate was incubated for 20 h at 37 °C in an incubator (Incubator Heraeus INSTRUMENTS, Germany). Subsequently, the suspension was transferred into 1.5 mL reaction tubes (SARSTEDT, Germany) and centrifuged at 3000 × g for 5 min using a centrifuge (Heraeus pico 21, Thermo Fisher Scientific Inc., Waltham, USA). Pellets were resuspended in 300  $\mu$ L fixative, consisting of 2.5% glutaraldehyde and 1% paraformaldehyde in 0.05 m HEPES buffer.

Fixed cells were again sedimented and mixed 1:1 with 3% low-melting point agarose at 40 °C. After solidification on ice, the agarose-embedded cells were post-fixed with 1% osmium tetroxide and 2% uranyl acetate, before they were dehydrated in ethanol and embedded in LR White resin (hard grade; The London Resin Co. Ltd., UK). After polymerization at 60 °C for two days, resin blocks were trimmed and sectioned with an ultramicrotome (Leica UC7, Leica Microsystems, Germany) at 60–70 nm thickness. Sections were collected on naked copper grids (300–400 mesh), contrasted with uranyl acetate and lead citrate, and covered with a thin layer of carbon. Imaging was done with a transmission electron microscope (JEM-2100, Jeol, Japan) operated at 200 kV and a CMOS camera (Xarosa, EMSIS, Germany) with 2560 × 1920 px.

*Genomic Analysis*: All genomic analysis (Illumina Sequencing, Nanopore Sequencing, and Minimum spanning tree analysis) were performed on the five isolates: DSMZ 20477<sup>T</sup>, DSMZ 17050, VRE-13, VVE-B-19, A17sv1.

Illumina Sequencing: For all five E. faecium isolates (DSMZ 20477 $^{\rm T}$ , DSMZ 17050, A17sv1, VRE-13, VVE-B-19), whole genome sequencing was performed using Illumina NovaSeq.

DNA was extracted with the DNeasy Ultra Clean Microbial Kit (Qiagen, Hilden Germany). After quality control check by the Invitrogen Qubit 3 Fluorometer (Thermo Fisher Scientific Inc., Waltham, MA, USA) all samples were sent to CeGaT (Tübingen, Germany) for whole genome sequencing. The library preparation was done with the Illumina DNA Prep kit. Sequencing was performed on a NovaSeq 6000 with  $2 \times 100$  bp paired-end reads, and a Q30 value of 92.30% was achieved. Demultiplexing of the sequencing reads was performed with Illumina bcl2fastq (2.20). Adapters were trimmed with Skewer (version 0.2.2) (Jiang et al. 2014). Quality trimming of the reads has not been performed. Trimmed raw reads were aligned using the Burrows-Wheeler Aligner (BWA-mem version 0.7.17-cegat). Using a proprietary tool, reads that aligned to more than one locus with the same mapping score and duplicated reads, which most likely originated from the same PCR amplicon, were discarded. Proprietary software was used for variant detection. Variant calling was performed in the target regions with +/- 30 base pairs. The quality of the FASTQ files was analyzed with FastQC (version 0.11.5-cegat). Plots were created using ggplot2 (Wickham 2009) in R (version 3.6.1) (R Core Team 2015).

For assembled genome-based analyses, Illumina reads were quality-controlled using FastP v0.23.3, [100] assembled using Unicycler v0.5.0, [101] and annotated using Bakta v1.4.0[102] using its full database v3.1. Antimicrobial resistance genes were detected using AMRFinderPlus v4.0.15. [103]

Nanopore Sequencing: DNA was extracted according to the manufacturer's protocol with the Wizard Genomic DNA Purification Kit (Promega, Germany). Barcoding, priming, and loading the MinION, was performed

**Keywords** 

with the labelling Rapid Barcoding Kit 24 (SQK-RBK114.24) and loaded onto a MinION flow cell (R10.4.1, Oxford Nanopore Technologies) and sequenced on a MinION Mk1B device (Oxford Nanopore Technologies). Sequencing runs were monitored in real-time using the MinKNOW software (v23.11.2, Oxford Nanopore Technologies).

Genomes were assembled and annotated with the open-source bioinformatics platform Galaxy (Version 24.2.3.dev0). The following tools were used: Flye, a *de novo* assembler (Galaxy Version 2.9.5+galaxy 1),[104] Prokka for annotation (Galaxy Version 1.14.6 + galaxy1), and NanoPlot for quality assessment of the obtained reads (Galaxy Version 1.14.6 + galaxy 1).

Minimum Spanning Tree Analyses: The molecular epidemiology was investigated with a validated core genome MLST (cgMLST) scheme, including 1423 target alleles, using the Ridom SeqSphere+ software, version 10.5.1 (Ridom GmbH, Münster, Germany). Isolates differing in ≤3 alleles were considered as clonally related.

Statistical Analysis: For statistical analysis, the two-sample Student's t-test was performed using SigmaPlot (version 14.5). The presented data are depicted by the arithmetic means with the corresponding calculated standard error. For comparison of groups, a two-sample, two-sided Student's t-test was performed, with an alpha level of 0.05. A p-value < 0.05 was considered statistically significant. Sample sizes are indicated in the respective figure legends.

# Supporting Information

Supporting Information is available from the Wiley Online Library or from the author.

## **Acknowledgements**

The authors thank Petra Kaiser for resin embedding of the bacteria and Lars Möller for transmission-electron microscopy. The authors would like to express great gratitude and honor to Ralf Möller, who is sadly no longer with us. His vision and dedication were fundamental in establishing this project. He supported it with all his motivation and effort, shaping the core of this project. ICP-QQQ instrumentation for this work was financially supported by Saarland University and German Science Foundation (project number INST 256/553-1).

Open access funding enabled and organized by Projekt DEAL.

#### **Conflict of Interest**

The authors declare no conflict of interest.

## **Author Contributions**

A.L.B., S.L., K.S., and S.M.T. supervised the project and provided input.; F.A. conducted the microbiological experiments and analyzed the data and wrote the manuscript with input from all authors.; A.S.A., D.W.M. and F.M.; A.H. and R.K caried out material functionalization. performed ICP-QQQ measurements; R.A. performed magnetron sputtering for coatings.; P.B. conducted additional microbiological experiments.; C.S. and M.L. performed scanning and transmission microscopy; O.S., P.G.H., K.X., and K.R. conducted sequencing and genome analysis; Sequencing and experimental support was provided by R.A.d.P. All authors contributed to data interpretation and manuscript preparation. All authors have read and approved the final version of the manuscript.

# **Data Availability Statement**

The data that support the findings of this study are available from the corresponding author upon reasonable request.

antimicrobial functionalized copper and brass surfaces, copper coatings, copper stress response, copper tolerance, Enterococcus faecium, vancomycin resistance

> Received: May 15, 2025 Revised: August 22, 2025 Published online:

- [1] H. W. Boucher, G. H. Talbot, J. S. Bradley, J. E. Edwards, D. Gilbert, L. B. Rice, M. Scheld, B. Spellberg, J. Bartlett, Clin. Infect. Dis. 2009,
- [2] X. M. Zhen, C. S. Lundborg, X. S. Sun, X. Q. Hu, H. J. Dong, Antimicrob. Resist. In. 2019, 8, 137.
- [3] K. Ravi, B. Singh, Bacteria 2024, 3, 76.
- [4] C. Aloke, I. Achilonu, Microb. Pathogen. 2023, 175, 105963.
- [5] S. W. J. Gould, M. D. Fielder, A. F. Kelly, M. Morgan, J. Kenny, D. P. Naughton, Annals of Microbiology 2009, 59, 151.
- [6] D. W. Müller, S. Lösslein, E. Terriac, K. Brix, K. Siems, R. Moeller, R. Kautenburger, F. Mücklich, Adv. Mater. Interfaces 2021, 8, 2001656.
- [7] A. L. Casey, D. Adams, T. J. Karpanen, P. A. Lambert, B. D. Cookson, P. Nightingale, L. Miruszenko, R. Shillam, P. Christian, T. S. Elliott, J. Hospital Infect. 2010, 74, 72.
- [8] A. N. Duckro, D. W. Blom, E. A. Lyle, R. A. Weinstein, M. K. Hayden, Arch. Intern. Med. 2005, 165, 302.
- [9] L. Porter, O. Sultan, B. G. Mitchell, A. Jenney, M. Kiernan, D. J. Brewster, P. L. Russo, J. Hosp. Infect. 2024, 147, 25.
- [10] M. Colin, F. Klingelschmitt, E. Charpentier, J. Josse, L. Kanagaratnam, C. De Champs, S. C. Gangloff, Materials 2018, 11, 2479.
- [11] M. G. Schmidt, H. H. Attaway, S. E. Fairey, J. Howard, D. Mohr, S. Craig, Appl. Environ. Microbiol. 2020, 86.
- [12] C. D. Salgado, K. A. Sepkowitz, J. F. John, J. R. Cantey, H. H. Attaway, K. D. Freeman, P. A. Sharpe, H. T. Michels, M. G. Schmidt, Infect. Control Hospit. Epidemiol. 2013, 34, 479.
- [13] J. Abraham, K. Dowling, S. Florentine, Materials 2021, 14.
- [14] S. L. Warnes, C. W. Keevil, Appl. Environ. Microbiol. 2011, 77, 6049.
- [15] G. Grass, C. Rensing, M. Solioz, Appl. Environ. Microbiol. 2011, 77,
- [16] L. Macomber, J. A. Imlay, Proc. Natl. Acad. Sci. USA 2009, 106, 8344.
- [17] C. Hahn, M. Hans, C. Hein, R. L. Mancinelli, F. Mücklich, R. Wirth, P. Rettberg, C. E. Hellweg, R. Moeller, Astrobiology 2017, 17, 1183.
- [18] A. H. A. Lutey, L. Gemini, L. Romoli, G. Lazzini, F. Fuso, M. Faucon, R. Kling, Sci. Rep. 2018, 8, 10112.
- [19] K. Siems, D. W. Müller, L. Maertens, A. Ahmed, R. V. Houdt, R. L. Mancinelli, S. Baur, K. Brix, R. Kautenburger, N. Caplin, J. Krause, R. Demets, M. Vukich, A. Tortora, C. Roesch, G. Holland, M. Laue, F. Mücklich, R. Moeller, Front. Space Technol. 2022, 2, 773244.
- [20] S. M. Timofeev, K. Siems, D. W. Müller, A. S. Ahmed, A. Schiele, K. Brix, C. L. Krämer, F. Arndt, R. Kautenburger, F. Mücklich, S. Leuko, Adv. Mater. Interfaces 2025, 12.
- [21] C. J. Blehm, M. S. G. Monteiro, M. C. Bessa, M. Leyser, A. S. Dias, J. Sumienski, S. W. Gallo, A. B. da Silva, A. Barros, R. Marco, C. P. Preve, C. A. S. Ferreira, F. Ramos, S. D. de Oliveira, AMB Express 2022, 12, 146.
- [22] S. Paton, G. Moore, L. Campagnolo, T. Pottage, Life Sci. Space Res. **2020**, 26, 125.
- [23] N. Bharadishettar, K. U. Bhat, P. DB, Metals 2021, 11.
- [24] D. M. Mattox, In Handbook of Physical Vapor Deposition (PVD) Processing, Elsevier, Amsterdam 2010.

, Wiley Online Library on [10/09/2025]. See the Terms

and-conditions) on Wiley Online Library for rules of use; OA articles are

governed by the applicable Creative Commons License



*A*DVANCED

- [25] D. Mitra, E. T. Kang, K. G. Neoh, ACS Appl. Mater. Interfaces 2020, 12, 21159.
- [26] A. Rebelo, J. Mourao, A. R. Freitas, B. Duarte, E. Silveira, A. Sanchez-Valenzuela, A. Almeida, F. Baquero, T. M. Coque, L. Peixe, P. Antunes, C. Novais, Sci. Total Environ. 2021, 787, 147548.
- [27] M. Imran, K. R. Das, M. M. Naik, Chemosphere 2019, 215, 846.
- [28] L. G. Li, Y. Xia, T. Zhang, Isme J 2017, 11, 651.
- [29] C. Vignaroli, S. Pasquaroli, B. Citterio, A. Di Cesare, G. Mangiaterra, D. Fattorini, F. Biavasco, *Environm. Pollut.* 2018, 237, 406.
- [30] C. Novais, A. R. Freitas, E. Silveira, P. Antunes, R. Silva, T. M. Coque, L. Peixe, J. Antimicrob. Chemother. 2013, 68, 2746.
- [31] X. T. Zou, M. W. Weng, X. Ji, R. Guo, W. J. Zheng, W. Yao, J Microbiol 2017, 55, 703.
- [32] European Food Safety Authority. EFSA reviews maximum content of copper in feed for piglets, 2016, https://www.efsa.europa.eu/en/ press/news/160809-0 (accessed Sept 1, 2025).
- [33] European Commission. Commission Implementing Regulation (EU) 2018/1039 of 23 July 2018 concerning the authorisation of Copper(II) diacetate monohydrate as feed additives for all animal species. Off J Eur Union L186: 3–24, 2018.
- [34] H. Hasman, F. M. Aarestrup, Antimicrob. Agents Chemother. 2002, 46, 1410.
- [35] R. G. Amachawadi, N. W. Shelton, X. Shi, J. Vinasco, S. S. Dritz, M. D. Tokach, J. L. Nelssen, H. M. Scott, T. G. Nagaraja, Appl. Environ. Microbiol. 2011, 77, 5597.
- [36] H. Hasman, I. Kempf, B. Chidaine, R. Cariolet, A. K. Ersbøll, H. Houe, H. C. Bruun Hansen, F. M. Aarestrup, Appl. Environ. Microbiol. 2006, 72, 5784.
- [37] M. Solioz, J. V. Stoyanov, FEMS Microbiol. Rev. 2003, 27, 183.
- [38] O. Nilsson, Infect. Ecol. Epidemiol. 2012, 2, 16959.
- [39] E. Silveira, A. R. Freitas, P. Antunes, M. Barros, J. Campos, T. M. Coque, L. Peixe, C. Novais, J. Antimicrob. Chemother. 2014, 69, 899.
- [40] D. W. Müller, T. Fox, P. G. Grützmacher, S. Suarez, F. Mücklich, Sci. Rep. 2020, 10, 3647.
- [41] A. S. Ahmed, D. Sancio, D. W. Müller, J.-F. Pierson, F. Mücklich, Mater. Today Adv. 2025, 27, 100596.
- [42] M. C. Díaz CC, P. L. Schilardi, S. G. de Saravia, M. A. F. L. de Mele, Mater. Res. 2007, 10, 11.
- [43] K. A. Whitehead, J. Verran, Food and Bioproducts Processing 2006, 84, 253
- [44] A. Peter, A. H. Lutey, S. Faas, L. Romoli, V. Onuseit, T. Graf, Opt. Laser Technol. 2020, 123, 105954.
- [45] C. Adlhart, J. Verran, N. F. Azevedo, H. Olmez, M. M. Keinänen-Toivola, I. Gouveia, L. F. Melo, F. Crijns, J. Hospit. Infect. 2018, 99, 239.
- [46] R. Helbig, D. Günther, J. Friedrichs, F. Rössler, A. Lasagni, C. Werner, Biomater. Sci. 2016, 4, 1074.
- [47] D. W. Müller, C. Pauly, K. Brix, R. Kautenburger, F. Mücklich, Biomaterials Advances 2025, 169, 214184.
- [48] J. Elguindi, S. Moffitt, H. Hasman, C. Andrade, S. Raghavan, C. Rensing, Appl. Microbiol. Biotechnol. 2011, 89, 1963.
- [49] K. Bondarczuk, Z. Piotrowska-Seget, Cell Biol. Toxicol. 2013, 29, 397.
- [50] N. Glibota, M. J. G. Burgos, A. Gálvez, E. Ortega, J. Sci. Food Agric. 2019, 99, 4677.
- [51] M. Ramsey, A. Hartke, M. Huycke, In, (Eds: M. S. Gilmore, D. B. Clewell, Y. Ike, N. Shankar) Enterococci, From Commensals to Leading Causes of Drug Resistant Infection, Massachusetts Eye and Ear Infirmary, Boston 2014.
- [52] M. M. Almoudi, A. S. Hussein, M. I. Abu Hassan, Saudi Dent J 2018, 30, 283.
- [53] A. Sirelkhatim, S. Mahmud, A. Seeni, N. H. Kaus, L. C. Ann, S. K. Bakhori, H. Hasan, D. Mohamad, *Nanomicro Lett* 2015, 7, 219.
- [54] J. Y. Long, M. L. Zhong, P. X. Fan, D. W. Gong, H. J. Zhang, J. Laser Applicat. 2015, 27, S29107.

- [55] D. W. Müller, B. Josten, S. Waeltermann, C. Pauly, S. Slawik, K. Brix, R. Kautenburger, F. Mücklich, Front. Mater. 2024, 11, 1397937.
- [56] A. S. Ahmed, D. W. Müller, S. Bruyere, A. Holtsch, F. Müller, J. Barrirero, K. Brix, S. Migot, R. Kautenburger, K. Jacobs, J.-F. Pierson, F. Mücklich, ACS Appl. Mater. Interfaces 2023, 15, 36908.
- [57] J. Q. Luo, C. Hein, J. Ghanbaja, J. F. Pierson, F. Mücklich, *Micron* 2019, 127.
- [58] D. A. Montero, C. Arellano, M. Pardo, R. Vera, R. Gálvez, M. Cifuentes, M. A. Berasain, M. Gómez, C. Ramírez, R. M. Vidal, Antimicrob Resist In 2019, 8, 3.
- [59] S. Liu, H. J. Guo, J. Iron Steel Res. Int. 2024, 31, 24.
- [60] S. M. Lösslein, R. Merz, Y. Rodriguez-Martinez, F. Schäfer, P. G. Grützmacher, D. Horwat, M. Kopnarski, F. Mücklich, J Colloid Interf Sci 2024, 670, 658.
- [61] A. Ganapathi, H. Krishnan, A. Kedharnath, Int. J. Sci. Eng. Applicat. 2013.
- [62] A. S. Valenzuela, N. Benomar, H. Abriouel, M. M. Cañamero, R. L. López, A. Gálvez, J. Food Protect. 2013, 76, 1806.
- [63] K. Acharya, S. Shaw, S. P. Bhattacharya, S. Biswas, S. Bhandary, A. Bhattacharya, World J. Microbiol. Biotechnol. 2024, 40, 270.
- [64] T. Hagi, M. Kobayashi, M. Nomura, FEMS Microbiol. Lett. 2014, 350, 223
- [65] A. H. RA, F. Triq, Biomedical & Pharmacology Journal 2012, 5, 51.
- [66] C. A. F. Portela, K. F. Smart, S. Tumanov, G. M. Cook, S. G. Villas-Bôas, J. Bacteriol. 2014, 196, 2012.
- [67] H. K. Abicht, Y. Gonskikh, S. D. Gerber, M. Solioz, *Microbiol-Sgm* 2013, 159, 1190.
- [68] K. S. Chaturvedi, J. P. Henderson, Front. Cellul. Infect. Microbiol. 2014. 4.
- [69] S. Mathews, R. Kumar, M. Solioz, Appl. Environ. Microbiol. 2015, 81, 6399
- [70] J. Mourão, J. Rae, E. Silveira, A. R. Freitas, T. M. Coque, L. Peixe, P. Antunes, C. Novais, J. Antimicrob. Chemother. 2016, 71, 560.
- [71] S. H. Egido, M. S. Ruiz, S. Ines Revuelta, I. G. Garcia, J. L. Bellido, New Microbes New Infect 2016, 9, 47.
- [72] S. Liu, X. X. Zhang, J. Medic. Microbiol. 2016, 65, 1143.
- [73] L. K. Harris, J. A. Theriot, Trends Microbiol. 2018, 26, 815.
- [74] K. Peters, M. Pazos, Z. Edoo, J.-E. Hugonnet, A. M. Martorana, A. Polissi, M. S. VanNieuwenhze, M. Arthur, W. Vollmer, P Natl Acad Sci USA 2018, 115, 10786.
- [75] T. Wagner, B. Joshi, J. Janice, F. Askarian, N. Skalko-Basnet, O. C. Hagestad, A. Mekhlif, S. N. Wai, K. Hegstad, M. Johannessen, J. Proteomics 2018, 187, 28.
- [76] R. Wirth, Eur. J. Biochem. 1994, 222, 235.
- [77] M. Rohde, Microbiol. Spectr. 2019, 7, 10.
- [78] T. P. Cushnie, N. H. O'Driscoll, A. J. Lamb, Cell. Mol. Life Sci. 2016, 73, 4471.
- [79] T. M. Wagner, A. K. Pöntinen, M. AL Rubaye, A. Sundsfjord, K. Hegstad, Clin. Microbiol. Infect. 2024, 30, 396.e1.
- [80] M. Arthur, R. Quintiliani, Antimicrob. Agents Chemother. 2001, 45, 375.
- [81] A. M. Hammerum, K. T. Karstensen, L. Roer, H. Kaya, M. Lindegaard, L. J. Porsbo, A. Kjerulf, M. Pinholt, B. J. Holzknecht, P. Worning, K. L. Nielsen, S. G. K. Hansen, M. Clausen, T. S. Søndergaard, E. Dzajic, C. Østergaard, M. Wang, K. Koch, H. Hasman, Eurosurveillance 2024, 29, 2300633.
- [82] G. Werner, B. Neumann, R. E. Weber, et al., Drug Resist Update 2020, 53.
- [83] M. Latorre, J. Galloway-Peña, J. H. Roh, M. Budinich, A. Reyes-Jara, B. E. Murray, A. Maass, M. González, *Metallomics* 2014, 6, 572.
- [84] W. van Schaik, J. Top, D. R. Riley, J. Boekhorst, J. E. Vrijenhoek, C. M. Schapendonk, A. P. Hendrickx, I. J. Nijman, M. J. Bonten, H. Tettelin, R. J. Willems, BMC Genomics 2010, 11.

) on Wiley Online Library for rules of use; OA articles are

governed by the applicable Creative Commons License

www.advancedsciencenews.com



www.advmatinterfaces.de

- [85] S. Zhang, D. Wang, Y. Wang, H. Hasman, F. M. Aarestrup, H. A. Alwathnani, Y.-G. Zhu, C. Rensing, Stand. Genom. Sci. 2015, 10, 35.
- [86] Y. Fujiya, T. Harada, Y. Sugawara, Y. Akeda, M. Yasuda, A. Masumi, J. Hayashi, N. Tanimura, Y. Tsujimoto, W. Shibata, T. Yamaguchi, R. Kawahara, I. Nishi, S. Hamada, K. Tomono, H. Kakeya, Sci. Rep. 2021, 11, 14780.
- [87] E. Sadowy, I. Gawryszewska, A. Kuch, D. Zabicka, W. Hryniewicz, Europ. J. Clinic. Microbiol. Infect. Diseas. 2018, 37, 927.
- [88] A. P. Tedim, V. F. Lanza, M. Manrique, E. Pareja, P. Ruiz-Garbajosa, R. Cantón, F. Baquero, T. M. Coque, R. Tobes, Genome Announc 2017,
- [89] A. R. Freitas, T. M. Coque, C. Novais, A. M. Hammerum, C. H. Lester, M. J. Zervos, S. Donabedian, L. B. Jensen, M. V. Francia, F. Baquero, L. Peixe, J Clin Microbiol 2011, 49, 925.
- [90] C. Torres, C. A. Alonso, L. Ruiz-Ripa, R. Leon-Sampedro, R. Del Campo, T. M. Coque, Microbiol Spectr 2018, 6.
- [91] Y. Ly-Sauerbrey, R. Anton, L. Kopruch, C. L. Krämer, A. L. Boschert, C. Neidhöfer, O. Schwengers, D. Zander, S. Leuko, Front. Microbiol. **2025**, 16, 1659828.
- [92] S. Rabow, M. Soares, J. Rousk, Journal of Applied Ecology 2023, 60,
- [93] J. O'Neill, Review on Antimicrobial Resistance. Antimicrobial Resistance: Tackling a Crisis for the Health and Wealth of Nations.: Review on Antimicrobial Resistance, 2014.

- [94] D. W. Müller, A. Holtsch, S. Lösslein, C. Pauly, C. Spengler, S. Grandthyll, K. Jacobs, F. Mücklich, F. Müller, Langmuir 2020, 36,
- [95] A. S. Ahmed, D. W. Müller, S. Bruyère, A. Holtsch, F. Müller, K. Brix, S. Migot, R. Kautenburger, K. Jacobs, J.-F. Pierson, F. Mücklich, Appl. Surf. Sci. 2024, 665, 160338.
- [96] S. M. Lößlein, M. Kasper, R. Merz, C. Pauly, D. W. Müller, M. Kopnarski, F. Mücklich, Practical Metallography 2021, 58, 388.
- [97] F. Arndt, K. Siems, S. V. Walker, N. C. Bryan, S. Leuko, R. Moeller, A. L. Boschert, Npj Microgravity 2024, 10, 103.
- [98] M. A. Downing, J. Xiong, A. Eshaghi, A. McGeer, S. N. Patel, J. Johnstone, J. Clinic. Microbiol. 2015, 53, 3951.
- [99] S. Mathews, M. Hans, F. Mücklich, M. Solioz, Appl. Environ. Microbiol. 2013, 79, 2605.
- [100] S. F. Chen, Imeta 2023, 2, 107.
- [101] R. R. Wick, L. M. Judd, C. L. Gorrie, K. E. Holt, PLoS Comput. Biol. **2017**, 13, 1005595.
- [102] O. Schwengers, L. Jelonek, M. A. Dieckmann, S. Beyvers, J. Blom, A. Goesmann, Microbial Genomics 2021, 7, 000685.
- [103] M. Feldgarden, V. Brover, N. Gonzalez-Escalona, J. G. Frye, J. Haendiges, D. H. Haft, M. Hoffmann, J. B. Pettengill, A. B. Prasad, G. E. Tillman, G. H. Tyson, W. Klimke, Sci. Rep. 2021, 11, 12728.
- [104] M. Kolmogorov, J. Yuan, Y. Lin, P. A. Pevzner, Nat. Biotechnol. 2019, 37, 540.